ALMA MATER STUDIORUM
UNIVERSITA' DI BOLOGNA

SCUOLA DI SCIENZE
Corso di Laurea Magistrale in
BIOLOGIA MARINA

Using sclerochronology to estimate the growth rate in *Pinna nobilis*: a case study of Les Alfaques Bay population (Ebro Delta, Spain).

Tesi di laurea in Alterazione e Conservazione degli Habitat Marini

Relatore	Presentata da
Prof. MARCO ABBIATI	SILVIA FRAISSINET

Correlatore

Dott. JOSÈ RAFAEL GARCÌA-MARCH

Sessione Unica Dicembre 2017
Anno Accademico 2016/2017

Summary

1. Introduction

1.1 General description

Figure 1 *Pinna nobilis*

The pen shell *Pinna nobilis* (Linnaeus, 1758) is a semi-infaunal pteromorphic bivalve, mollusks belonging to the Pinnidae family containing three genera, *Pinna*, *Atrina*, and *Streptopinna*. Reaching a size of up to 120 cm (Zavodnik et al., 1991), *Pinna nobilis*, is the largest bivalve of the Mediterranean Sea (where it is endemic), ranks amongst the largest in the world, and may live over 37 years (http://www.pinnanobilis.free.fr). It occurs at depths between 0.5 and 60 m, mostly on soft-bottom overgrown by seagrass meadows, but also occasionally on bare sand (Garcìa-March et al., *2002*; Katsanevakis, 2007b; Zavodnik et al., 1991). Attachment, as is the case for many other Pteriomorphia, is achieved by byssus threads, which are glued to pebbles, sand, small pieces of hard detritic material, and roots and rhizomes of *P. oceanica* (Garcìa March 2005). Known since antiquity, this bivalve mollusc suffered intensive human exploitation, the ancient Romans fished it to extract the so-called "sea silk" which was a precious commodity, yet the Islamists used the shell to make tools or small jewels, and in many Mediterranean countries it has long been considered a delicious dish. Anthropic pressure on this species has never been as high as in recent decades due to habitat degradation, illegal trawling, coastal construction, boat anchoring, and pollution. All these anthropogenic and environmental threats contributed to accelerating the decline of populations in the Mediterranean Basin (Basso et al., 2015). To preserve the existing populations of *Pinna nobilis*, this species has been included in Annex IV of the European Council Directive 92/43 / EEC (1992) and in Annex II of the Barcelona Convention. This species is also protected under local law in all European Union Mediterranean countries. Despite conservation efforts, *Pinna nobilis* populations continue to decline, and recently the situation has worsened, due to the introduction into the Mediterranean of parasitic alien species transported by ballast waters of transoceanic merchant vessels.

1.2 Shell.

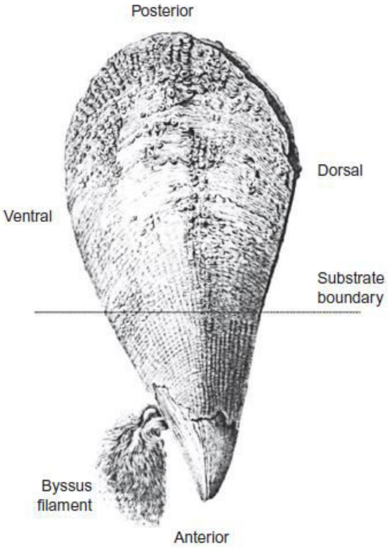

Figure 2 General drawing of an adult individual pen shell, *Pinna nobilis*, as it is commonly observed, with the tapered anterior third of the shell buried in the sediment and attached to the substratum by byssus threads. (credits Basso et al 2015).

Most of the mollusks have developed a rigid calcified exoskeleton - the shell - to protect themselves against environmental pressures and predators. The shell is an organo-mineral construction, in which the mineral phase usually represents more than 95% of the weight, and the organic fraction, less than 5%. (Lowenstam & Weiner 1989). Shell construction begins in the early life stages of the individual, and its growth is, more or less, continuous throughout their life. The structure responsible for the mineral deposition and shell formation is the mantle, the thin epithelium that envelops the soft body of mollusks and which is in contact with the growing shell. (Marin et al., 2011). The trochophore larvae, produces an organic lamella, which provides support for subsequent mineralization. Later, during ontogenic development, this organic lamella becomes the periostracum, the skinny outer layer of the shell. Among the adult specimen, the shell growth takes place at the border of the shell, in a minute space sealed by the periostracum and the calcifying mantle (Marin & Luquet 2005). In that extrapallial space, the mineral cells of the calcifying mantle release all the precursors for mineralization, the mineral ions, mainly calcium and bicarbonate, which are actively extruded from the cytoplasm by ionic pumps, and some minor elements such as magnesium or strontium and the organic components of the shell matrix, such as proteins and polysaccharides which are secreted by exocytosis. These shell matrix components represent a mixture of proteins, glycoproteins, acidic polysaccharides and chitin (Marin & Luquet 2005). The shell of the Pinnidae family has thick and solid valves. Shells are variable in shape from triangular to hatchet-shaped or subglobular (Silina 2011). The color of the shell is translucent light brown for juvenile specimens and becomes opaque brown-red in the adults. Like several bivalves of

Mediterranean or temperate zones, shell growth in *P. nobilis* follows a seasonal pattern, the shell grows slowly during the cold months and has a maximum growth rate during late spring and early summer (Katsanevakis 2007). When the water temperatures exceed a critical threshold (around 29° C), the shell growth slows down or stops. The shells of young specimens are characterized by the formation of thin calcitic hollow spines, produced by the pleated border of the mantle. These spines, which are extremely sharp, fragile and brittle, are regularly distributed on the entire outer surface of the two valves, according to the shell growth lines, making difficult to distinguish a juvenile of *Pinna nobilis* by an adult *Pinna rudis*. When aging, they are progressively eroded (Cosentino and Jacob 2006). The shell of *P. nobilis* exhibits a bilayered calcified structure, which means that the mantle epithelium that produces the shell is not homogeneous: the epithelial cells located at the border of the mantle are dedicated to the deposition of the prismatic layer while the epithelial cells are located more proximal from the shell tip secrete the nacre layer (Marin et al., 2011). The outer mineralized layer is calcitic and composed of "simple" prisms, developed perpendicularly to the surface of the shell. The inner layer is light gray and made by aragonite. It exhibits the iridescence characteristic of nacreous textures. While the outer prismatic layer covers the whole shell, the nacreous layer is restricted to the area between the adductor muscle scars, which represents about one-half of the shell height (Fig.3) (Marin et al., 2011).

Figure 3 Nacreous layer (nl)

1.2.1 Periostracum

The periostracum is the shell protein's outer layer, it is visible in juvenile individuals but is rapidly eroded during the growth process. It is made up of quinone tanned scleroproteins. The scleroproteins have the function of contributing to the solidity of the organic structures built by the animals, in this case, the shell, are also characterized by a high resistance to proteinases and hydrolytic solvents. In fact, the periostracum has a protective function in forming a waterproof covering of the shell and preventing the corrosion of the calcified shell by the acidic waters (Taylor & Kennedy 1969), as well as being a support for the growth of the outer layers of the shell.

1.2.2 Prismatic layer

After the production of an initial amorphous material in the extrapallial space, the formation of the prismatic layer, starts inside the organic lamella. *Pinna nobilis* has simple calcite prisms (Fig. 4), arranged with their crystallographic c axes normal to the layer surface (Taylor et al., 69). The prisms are larger than in any other family (up to 1 mm) (Marin et al., 2011). They are also first-order prisms, mutually parallel, adjacent structural units that do not strongly interdigitate along their mutual boundaries (Carter and Clark 85). This kind of prisms are generally longer than thicker, oriented with the axis of the length perpendicular to the shell plane. They are defined as regular simple prismatic structures, in which each 1st order prism is columnar and has a more or less equidimensional (non-elongated) polygonal cross-sectional shape (Marin et al., 2011). When observed in cross-section, the prisms of *P. nobilis* exhibit a polygonal shape, usually penta- heptagonal. Consequently, in the surface view, the prismatic layer exhibits a typical "honeycomb" structure pattern (Taylor et al., 1969) (Fig. 5), with the prisms maintained by an interprismatic insoluble organic sheath, that some authors assimilated to conchiolin (Gregoire 1967). The unusual size of *P.nobilis* prisms and a large number of scleroproteins contained in them give a flexible nature to the outer layer. This flexibility allows the outer layer of calcite to adjust the opening of the shell when the posterior adductor muscle is relaxed. (Garcia-March 2007).

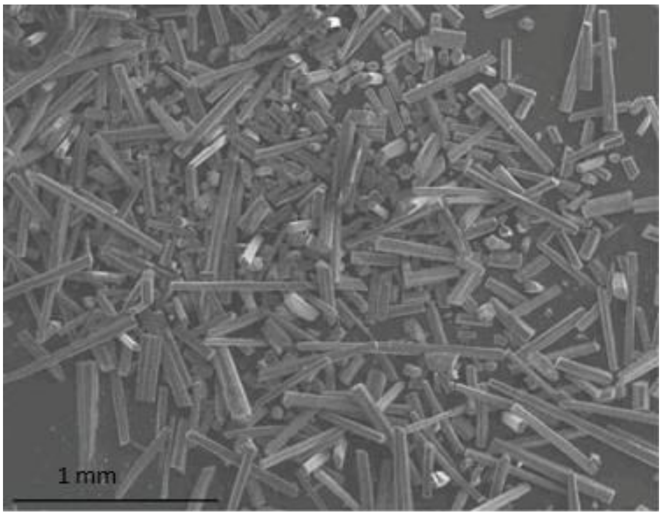

Figura 4 single calcitic prisms

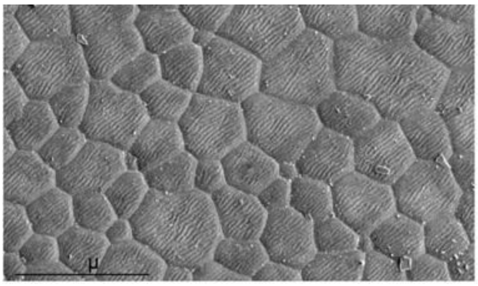

Figure 5 Honeycomb structure pattern

1.2.3 Nacre layer

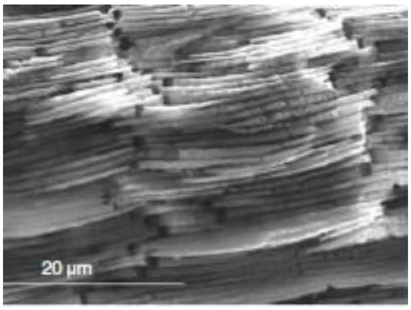

Figure 6 Cross section through the nacreous layer. The nacre exhibits the typical “row stack nacre” microstructure, observed in the Pinnidae family.

The nacre of *Pinna nobilis* is defined as a "row-stack nacre" (Fig. 6) (Wise 1970, Carter and Clark 1985) and is described as a "nacreous structure in which mutually parallel elongate tablets show vertical stacking in vertical sections perpendicular to their length axes; brick wall and / or stair stacking in vertical sections parallel to their length axes. Row stack is a well-developed in *Pinna nobilis*, where it enhances directional flexibility of the shell. The transition zone between the prismatic and the nacreous layer is rather abrupt (Cuif et al., 1985). It is marked by the formation of an intermediate layer, about 50 mm thick, this intermediate brownish layer is essentially organic and insoluble (Marin et al 2011). In young specimens (2-3 years old), the nacre layer is extremely thin (not more than 2-3 mm) and translucent. In old specimens (> 20 years), the nacreous layer is opaque and reaches a thickness of about 10 mm in the anterior tip (Marin et al., 2011). Close observation of these layers in thin sections of a radial cut of the shell shows that the nacre is deposited in two steps, in the inner side of the shell. Firstly, the first nacre layer (n1) (Garcìa-March and Marquez-Aliaga, 2007; Garcìa-March et al., 2011) is deposited covering the calcite. The second nacre layer with the same characteristics is deposited, covering the myostracum in the anterior part of the shell, growing in the posterior direction with ontogeny (n2) (Garcìa-March and Marquez-Aliaga, 2007; Garcìa-March et al., 2011), this layer is tapering more and then becomes a slim n1 of the earlier part.

1.2.4 Myostracum

The myostracum of the posterior adductor muscle scar (hereafter PAMS) is a continuous thin aragonite layer covering the nacre where the muscles attach to the shell (Basso et al 2015). It is possible to observe it in the dorsal lobe of the nacre, except where it is covered by layer n2. Observing a radial section we notice that the myostracum starts from the posterior tip of the last PAMS, covering the layer n1 in the inner part of the shell. The myostracum forms the innermost layer for about half the extension of the nacre dorsal lobe. Then it is covered by the layer n2, is immersed completely in this layer which becomes progressively thinner, then converted to n1 in the front. (Fig. 7)

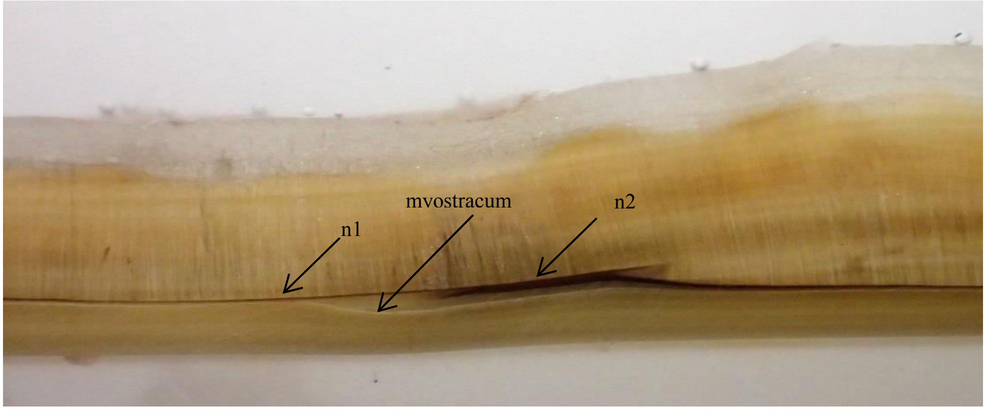

Figure 7 Thin sheet of the inner register (IR) of *Pinna nobilis* at the level of posterior adductor muscle scars (PAMS).

1.2.5 Internal register

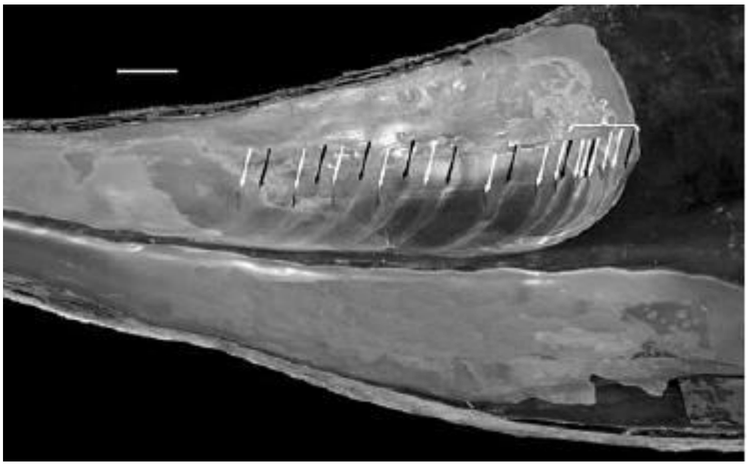

Figure 8 Dorsal nacre lobe of the right valve of *Pinna nobilis* showing posterior adductor muscle scars (PAMS). Black arrows mark the position of the straight lines (SL), white arrows mark the position of the rings (R).

The posterior adductor muscle leaves clear marks on the shell interface PAMS which consist of a series of straight lines and rings in the dorsal lobe nacre (Fig.8). The position of these signs can vary among adult individuals of the same population (Garcia March & Aliaga 2007). By cutting the radial section along the PAMS it is possible to note the signs of the internal register formed in the limit between the external calcitic and the internal nacreous layer and consist of (1) a short tongue of nacre located within the calcite prisms and directed towards the posterior of the shell, and (2) two strips of calcite prisms, one starting from the tongue and the other from the top of the tongue, both of them directed towards the posterior. The latter two are distinguished under the normal light by their different colors (bright and dark) (Garcia March & Aliaga 2007) (Fig. 9). The nacra tongues can be clearly visible, or still in formation. Partially formed nacre tongues are always observed in early winter (November-December) and early summer (ie July), implying that the growth of nacre in spring months is very low or absent. A fully formed nacre tongue is the result of two cycles of deposition occurring between late summer and early winter, but corresponding to two consecutive years. When nacre growth is resumed in midsummer after the winter growth break, it starts at the front of the previously deposited nacre completing the previous nacre tongue and increasing its width. The new nacre continues to grow in the posterior direction until December, forming a new wedge of nacre with myostracum intrusion when the annual growth cycle ends. Young individuals are an exception to this rule because they do not show winter growth breaks (Katsanevakis, 2007; Richardson et al., 1999) and hence do not form nacre tongues.

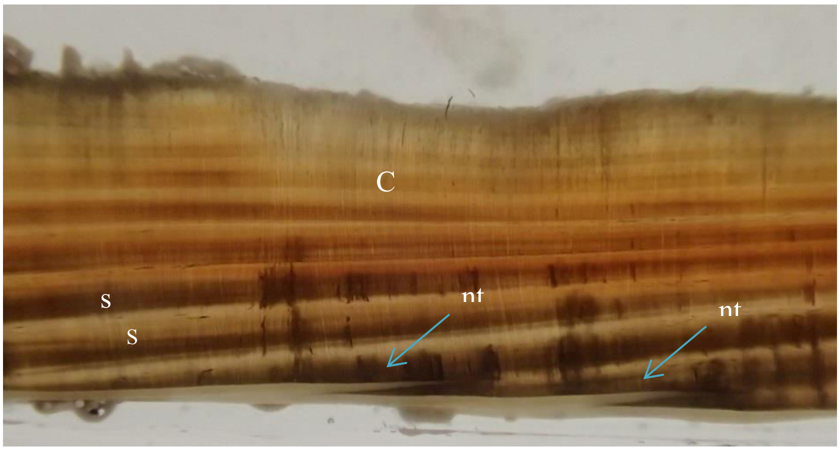

Figure 9 Internal register: nacre tongues (nt), black and white stripes of calcite (s), calcite (C).

1.2.6 Growth

Several methods were proposed for calculating the age of *Pinna nobilis*, starting with Moreteau and Vicente that in 1982 determined the age of a French population (Port-Cross) using the brands left by PAMS, assuming two consecutive marks are deposit in similar time, and that there is a relationship between the total height of the shell (Ht), and the distance between the last brand and the tip of the shell. They concluded that mollusk grows very fast in the first two years of life and subsequently drastically slows down the process, and estimated that a *P. nobilis* of about 20 cm was approximately 2 years old. Later, Richardson et al. (1999), carried out a study on the growth of *Pinna nobilis*, using stable isotopes. As they noted that in the *P. nobilis* smaller than 25 cm, the first deposition ring of PAMS could not be identified since it is known, that the first deposited ring in temperate bivalves is weak in definition and notoriously difficult to locate (Richardson et 1980, Richardson 1993). Similarly, the first ring on *P. nobilis* may be weakly defined. They highlighted the need to understand the periodicity of the PAMS rings and if the first ring settled in the first year of growth. Therefore, if the rings have an annual periodicity, then estimation of the age of the pinnids and inferred shell growth rates can be determined from the measurements of the space between the rings (Richardson et al., 1999). The stable oxygen isotope composition (δ_{18}O carbonate) of molluscan shell calcite can be used as a proxy for the ambient temperature and isotopic composition of the seawater if the calcite is precipitated in equilibrium with seawater (Urey 1947; Wefer and Berger 1991). They identified a seasonal pattern of deposition of PAMS, corresponding to an increase in water temperature at the beginning of summer, confirming the assumption of annual deposition of Moreteau and Vicente. Having the relationships of PAMS with total size and, PAMS with age, growth curves could be calculated using length-at-age data. They also noted that the first year after the settlement was actually characterized by rapid growth, with a peak in the summer, but in the second year, growth slowed dramatically, and this second year of growth coincided with the formation of the first PAMS ring. Concluding that, the first year could not be identified and that it would be added to the calculation obtained from the visible rings, and that in older specimens probably the second ring could also be lost. Therefore, the exact age was uncertain due to the criticalities in identifing the first years.

In 2007, García March and Marques Aliaga identified the internal register (IR) as an interesting option for determining age and to overcame the criticalities of the previous methods. Starting from PAMS in which rings (R) and straight lines (SL) are identified, they noted that the internal marks did not coincide with the PAMS rings, but that these SLs are the only visible traces of the IR. As a consequence, the SLs are not part of PAMS but are formed independently before the posterior adductor muscle arrives at their position (Garcia March and Marquez Aliaga 2007). Moreover, the mismatch between the number and position of the rings as compared to the internal register, as well as the brands hidden in older individuals, showed the existence of IR anterior to the last R, can be observed (Garcia March and Marquez Aliaga 2007). During this study, they also noted that two individuals had an internal register formed only by calcite strips, which coincided with the SLs, and were slightly dislocated respect to the rings. This observation confirms that two calcite strips without nacre tongue are also the evidence of an SL (Garcia March and Marquez Aliaga 2007). The calcite is layered predominantly between spring and early autumn, in the western Mediterranean (Garcia-March 2006). Garcia March and Aliaga suggested that each mark of the IR shows a switch in the mineral deposition, predominantly nacre between winter and early summer and calcite between summer and early autumn. Therefore this layering would indicate 1 year of age. The authors supposed that the experiment with Richardson's isotopes in 1999 actually reported the SLs and not the rings as considered by the author. Age determination using internal register showed different results compared to those obtained with PAMS. There is weak relationship between the IR and the R positions. The IR is generated at the boundary between the dorsal nacre lobe and calcite, an active shell-growing zone. The R is formed around the posterior adductor muscle, in relation to the posterior migration of the muscle (Kennedy et al., 2001). This explains why some marks of the IR can be observed in a more posterior position than the R. Considering that the number of obscured marks is variable among individuals depending on the age and degree of posterior migration of the tissues, newest SL can be layered under the other in the most posterior boundary of the dorsal nacre-lobe in old specimens, and that the newest R and SL are easily confused in mature individuals. So using the external register for determining the age of *Pinna nobilis* it can lead to errors, also because of the simple erosion of the apex of the shell the relationship with the total size can be distorted. In 2011 García March and Marquez-Aliaga confirmed the protocol based on the internal register to determine the age of *Pinna nobilis*, and proposed a new method for estimate the lost years due to the fact that the calcite layer in the anterior part is often incomplete, especially in adult individuals. Using the calcite thickness present in the older 3-4 increments, the underlying hypothesis was that the width of calcite at each annual increment is a function of the age because calcite stops growing when the nacre covers it on the inner side of the shell (Garcìa-March et al. 2011). The rationale of using the calcite width to estimate the anterior abrasion is the following: if, for example, the shell of an adult had lost 3 increments due to calcite abrasion, the width of the calcite at the first observed increment should be greater than that of the first one of the juvenile specimens, and should be similar to the width of the fourth of the juveniles. (Garcia March and Marquez Aliaga 2011). This work provides a new methodology that minimizes the resources needed for the development of growth studies in *Pinna nobilis*. Using this methodology, it is possible to sample many populations and collect empty shells in a single field survey and then complete the growth studies in the laboratory, saving a huge amount of time and resources. (Garcia March and Marquez Aliaga 2011). This will provide significant benefits for the understanding of the biology and ecology and conservation of *P. nobilis* populations.

1.3 Biology and ecology

1.3.1 Feeding

The *Pinna nobilis* is inserted with a third of its shell inside the substrate, while the posterior end of the shell projects in the water column. The species is a suspension feeder, taking in water through the inhalant siphon at the posterior end of the body. Several studies have been carried out on *Pinna nobilis* feeding, revealing that they ingest a wider range of food resources mainly debris (about 95% (Basso et al 2015)), but also phytoplankton and zooplankton. There was also an interesting relationship between the type of ingested food and the size of the mussel. In smaller individuals there is a greater amount of debris, than floating phytoplankton and zooplankton, compared to that found in larger specimens. Probably this is due to the fact that small-scale or juvenile individuals are closer to the substrate, or surrounded by *Posidonia*'s fronds, while the larger ones protruding the shell can benefit most from the water column, they ingested proportionately much greater quantities of diatoms, that were characteristic of water plankton, than did small fan shells. Conversely, the relative intake of bivalve larvae and dinoflagellates was significantly higher in small fan mussels. Throughout, the findings for medium-sized *P. nobilis* tend to be intermediate between those for small and large fan shells, confirming a highly significant pattern of differential food item intake (Devenport et al., 2011). There is also present in this mollusk, as in many other, a cannibal behavior towards their larvae and those of other species. In some cases, as many as 50% of potential settling mussel larvae are consumed by adult mussels, with significant implications for recruitment and population dynamics (Porri et al., 2008). *Pinna nobilis*, especially small specimens, consumed large numbers of bivalve veliger larvae (Devenport et al 2011).

1.3.2 Reproduction

The pen shell is a successful hermaphrodite, with an asynchronous gamete maturation (De Gaulejac et al., 1995b, c), which avoids self-fertilization. Sexual maturity is reached by 2 years of age (Richardson et al., 1999), with gametogenic development occurring from March to June followed by a succession of alternate spawning and fast gametogenesis from June to August (De Gaulejac, 1995). The pen shell, *P. nobilis*, has a dispersal phase with pelagic larvae, a possible weak spot for the population because early life stages of marine organisms, and in particular eggs and larvae, are considered the most vulnerable to environmental extremes. No studies on the survival of the planktonic stages of *P. nobilis* have been conducted and the mortality of larvae is virtually unknown in Pinnidae (Katsanevakis 2007b). Following the fertilization, a small veliger larva develops, which can be transported by the currents. The duration of the larval phase in *P. nobilis* lasts between 5-10 days. Settlements generally occur in sandy substrates close to seagrass bads, depending on the flow of currents, specimens may be very distant from the source population, resulting in a metapopulation. Soon after settlement, the new benthic *Pinna* is extremely small and fragile (Fig. 10). At settlement the postlarva is slightly over 1 mm in length, even at 1- 2 cm the shell is very fragile and the attachment is weak. At this stage, the animals are vulnerable to a range of risks, including those that are eaten by predators such as gastropods, cephalopods, asteroids and fish, and of being unable to feed effectively because of movement of the sediment or (as for the planktonic larvae) because the supply of suspended food is too diluted (Butler et al 93). Survivors in

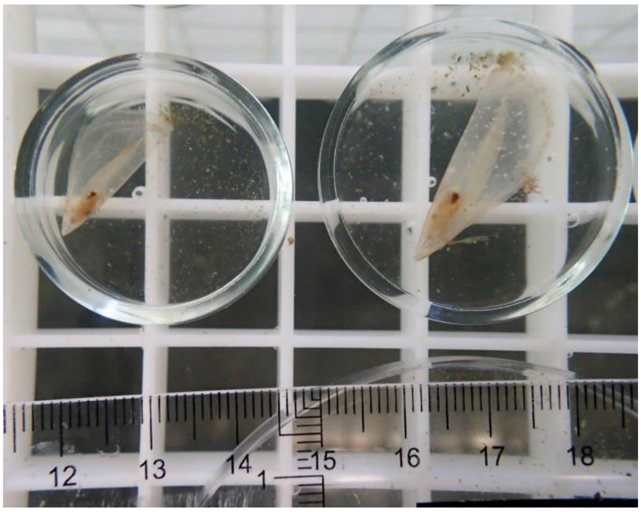

Figure 10 Larvae of *Pinna nobilis* in the veliger stadium

these phases grow rapidly and when they reach a size of about 10 cm, they are in a sufficiently far from the substrate to begin to show adult behavior. There is little known about the life cycle and the nutritional preferences of the larval phases of *Pinna nobilis*, these aspects are still being studied.

1.3.3 Gaping activity

The gaping activity of *Pinna nobilis* is strongly linked to physiological phenomena such as breathing and nutrition, but it is also a response to external stimuli. *Pinna nobilis* shows a rhythmic pattern of opening and closing of the valves, the main movements are concentrated at sunrise and at sunset. In general, specimens always closed the valves with sunset and followed the daily evolution of the Moon with their rhythms of gaping. The repetition of patterns makes it possible to distinguish between two main behaviors: (1) night-closing related to sunset and (2) night-opening related to the Moon, visible in the sky with the disc illuminated more than 50%. Another two less common trends were also observed: (3) day-closing and (4) night-opening with no visible moon (Garcia March et al 2008). Even some disturbance phenomena such as a severe storm or the passage of boats can promote the closing of the valve. *Pinna nobilis* can also respond to stress factors such as excess suspended particulates due to the movement of the water mass by closing the valves, or otherwise increasing its movement to clean the pallium cavity from the sediment (García March et al 2008).

1.3.4 Interaction with other species

Figure 11 Shell of died specimen o *Pinna nobilis* covered by epibiontes

The fan shell plays an important ecological role, providing new hard substrates to colonize, increasing the spatial heterogeneity of the surrounding softbottom communities, and contributing to the overall increase in the local biotope complexity level (Fig. 11).For some authors such as Raboui (2009) a fauna structure associated with the shell, is correlated with the lagoon-sea gradient and the biogeographic (longitudinal-longitudinal) gradient. Other authors such as Jacob (2002) are instead of the opposite view, believing that the size of the shell is bound to the specific wealth of colonizers. However, the presence and the type of moving and sessile organisms on the substrate offered by the *Pinna nobilis* shell is comparable to that of any hard substrate, with mollusks, annelids, crustaceans, ascidians, sponges, cnidarians, echinoderms, and bryozoans, in addition to algae. (Fig. 12). Moreover, the degree of complexity with regard to substrate-species relationships is very high, in fact, seen in the first, second and third order, where third-order species are growing on second-order ones that are themselves growing on Pinna's shell (Giacobbe 2002).

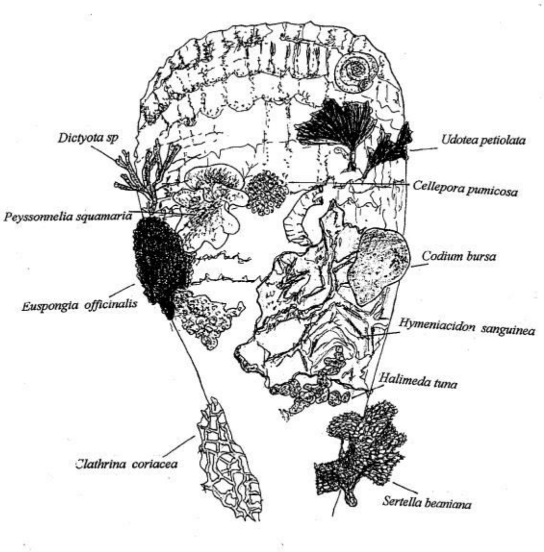

Dibujo: Carmen Barberá Cebrián.

Figure 12 schematic drawing of the most common epibiontes that can be found on the shell of *P. nobilis*. (credits Barbera 1996).

Moreover, *Pinna nobilis* frequently hosts the *Pontonia pinnophylax* (Fig. 13), a decapod crustacean, usually large individuals housed large crustaceans and vice versa. (Richardson 1997) They are typically found in adult couples but rarely even solitary males have been found inside the fan mussel.

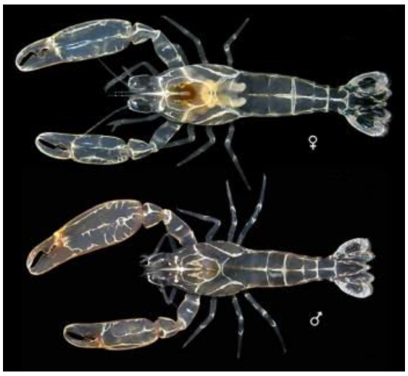

Figure 13 *Pontonia pinnophylax*

As regards the relationship between these two species, the presence of the shrimp at the edge of the shell close to the mantle (Fig. 14) may help to prevent predators, such as fishes frequently present in the *Posidonia* meadow, from attaching the delicate clots of the mollusks. What the *Pontonia pinnophylax* obtains from the relationship is less clear, they may be inquilines obtaining safety and shelter within the shell valves (Richardson 1997), a further possibility is that the shrimp consume the material that accumulates inside the cavity of the *Pinna nobilis* mantle. Calafiore et al (1991) suggests that probably the life cycles of the two species were related, in fact, in a study of the zoeal

Figure 14 *Pontonia pinnophylax* hidden inside the *Pinna nobilis* valve

Figure 15 Small individual of *P. nobilis* hidden in the leaves of *Posidonia oceanica.*

development of *P. pinnophylax*, it was found that development from zoea stage to post-larval stage only occurred in the presence of adult mussels, in the absence of *Pinna* the zoea continued to grow but did not metamorphose into juvenile shrimps.

Another interesting interaction is the *Pinna nobilis* exhibition with the *Posidonia oceanica*, its typical habitat. *Posidonia oceanica*, in fact, offers mollusk sword protection. Under high flow rates, high-density meadows generally attenuated drag forces on large shells but had little attenuating effect at low velocities and medium shoot density, while at high water speeds, large shells suffered from increased drag due to the deflection of the plants and augmented flow velocities above the canopy (Hendricks 2011). Mainly protected are small individuals that are completely covered by *P. oceanica* fronds, larger individuals with longer shells are more exposed to hydrodinamism. The influence of hydrodynamic facilitation of *P. nobilis* by *P. oceanica* meadows may well explain the size distribution of fan mussel populations with shallow sites being dominated by small individuals and large individuals were mostly observed in deeper or sheltered locations (García-March 2005) (Fig. 15 and 16).

Figure 16 Specimen large enough to emerge from the *Posidonia oceanica* leaves

1.4 Current situation

Pinna nobilis is one of the Mediterranean endangered species, and it is integrated into protection and monitoring programs at European level and by single states, to ensure its survival and well-being. Unfortunately, despite the efforts of protection, a mass-mortality event (MME) impact on the *Pinna nobilis* bivalve, it was detected in a wide geographic area of the Mediterranean Sea (W) in early autumn 2016 (Vázquez-Luis, 2017). Histological examination of affected individuals revealed the presence of a haplosporidian-like parasite within the digestive gland, was probably the pathogen that causes this mortality (Garcia March et al 2017). The parasite prevents the animal from feeding and this causes an arrest of growth, influences the stimulation response, the closing of the valve is slow or absent, mantle recession, emaciation and the occurrence of abundant large vesicles full of liquid on the visceral mass. The protozoa reproduce within the mollusk feeding on its tissues and bringing it to death. *Pinna rudis*, who shares the same habitat with *P. nobilis*, is not affected by this parasite, seems to be completely immune to it, and in fact, it is presently far more abundant than before because space and resource competition is at the moment strongly diminished.

This parasite reached the Mediterranean following the phenomenon that has been evolving ever since the introduction of alien species in this basin. The problem of ballast water has been felt since the late 1980s. The International Marine Organization, a specialist in maritime safety and marine pollution prevention, rose the issue, and laid to lay the foundations for the International Convention for the Control and Management of Ballast Water, approved in 2004. This is a document that forces ships to trace the use of these cargoes and which, over time, intends to impose on ship owners the installation of an onboard treatment system. The objective is to avoid the colonization of port waters by allochthonous species. They are transported by merchant ships in ballast water, but also attached to the keel of the ship itself, and often find themselves in the ports, but recently, as reported the University of Pavia in a study published by Biofing (Ferrario et al. 2017), even in mainly tourist areas, there was a strong presence of alien species, which indicates that even yachts, sailboats, and all the sporting sectors are involved in this worrying phenomenon. Some countries in the world such as Australia have rigid rules and restrictions for the entry of boats into their ports, they cannot access it with the keel covered with incurable epibionts. In the Mediterranean Sea, such regulation is blander, and to this, we add that significant changes have been made to the topographical structure of the territory. The enlargement of the Suez Canal, for example, has made access much easier, the species of the Red Sea entering the Mediterranean, expanding and multiplying rapidly, are endangering our flora and fauna, as well as human health, as they are often poisonous or nursing species. The Mediterranean is also accessible through the Strait of Gibraltar, which provides a connection with ocean waters, and an entrance corridor for Atlantic species.

The current situation on the Spanish' coast is worrying, after the first records of massive mortality of *Pinna nobilis*, many others events have been recorded. In early autumn 2016 (end September and early October 2016) an abnormally high mortality of *P. nobilis* individuals was observed almost simultaneously at several points in the Mediterranean Sea (SE) separated by hundreds of kilometres. (Garcia March and 2017). Since then the number of such events has grown, and the area of distribution has expanded. In the following months mortality has reached 100% in most of the southwest coast of Spain (Fig 17).

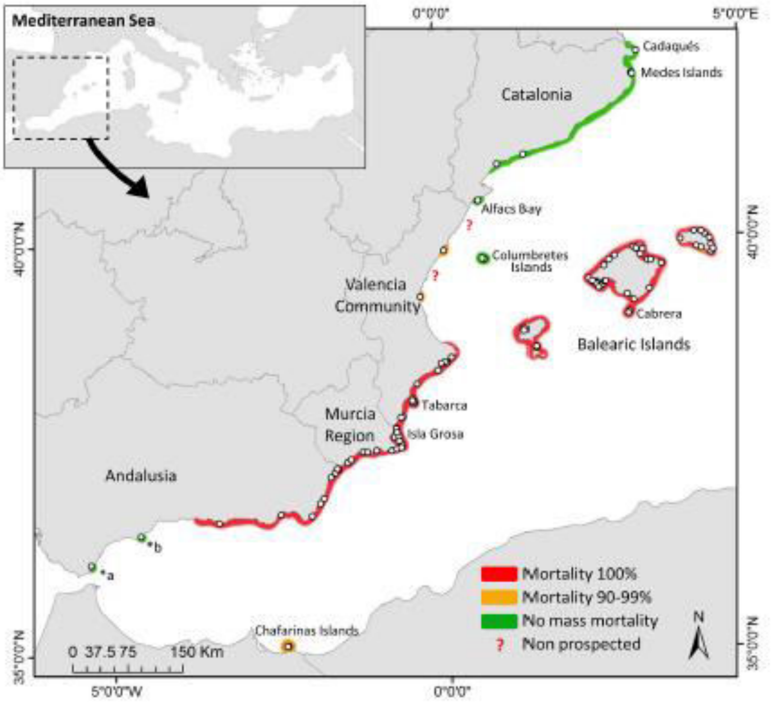

Figure 17 Map of the southwest coast of the Spain, with highlighted in red the zones where the mortality of the *Pinna nobilis* was of 100%.

The Catalan coast seems to be less affected by this dangerous phenomenon, and there are still records of living individuals. Unfortunately, this protozoan is spreading rapidly. In fact, it has also reached the coasts of Italy, the Ministry of Environment has called the protected marine areas to pay attention, and the operators of these bodies during the summer invited tourists, divers, diving center owners to contribute to this monitoring, reporting any sightings of dead individuals. Unfortunately, it would seem, that, the island of Ischia in Campania has been heavily affected by this massive mortality, and the percentage of *Pinna nobilis* has been drastically reduced. Even some coasts in southern France have reported massive mortality events by *P. nobilis*.

Figure 18 and 19 Posidonia oceanica meadow before and after the parasite in Calpe, Alicante coast (Spain).

The phenomenon, therefore, seems to be constantly expanding and it is hard to see a way to stop it (Fig 18,19).

Now, Spain intends to implement an emergency plan, collecting alive, presumably healthy, specimens from the not yet affected Catalan coasts, with the aim of studying its characteristics, proving a captive reproduction, and subtracting it from a possible contagion.

The situation is certainly very worrisome, attention should be paid to this massive extinction, which could to eradicate this endemic species from our sea forever. It would be opportune, and beneficial to act together, cooperating among the various states involved in seeking a quick and effective solution that could save *Pinna nobilis* from extinction, and which will enable us and future generations to enjoy it.

2. Aim of the project

The aim of this study is to quantify the growth rate of *Pinna nobilis* population by Les Alfaques Bay using an innovative method based on sclerochronology. This approach, by analyzing the internal register in adult specimens, allows the identification of the positions of PAMS masked by nacre and the estimation of the annual missing records. Thus, it's possible to provide more accurate estimations of the age and of the growth rate of individuals, compare to previous studies, even when some size classes are missing. Moreover, by estimating the growth rate on dead shells, this method complies with the conservation standards for this endangered species, avoiding the need for long-term and costly field measurements or isotopic studies. A size-age model was developed to support field studies and conservation strategies for *Pinna nobilis*.

3. Material and methods.

In this study, were analyzed 35 shells of *P.nobilis* collected in Les Alfaques Bay, Ebro Delta in Spain, at a depth between 1,3 and 3 meters. Dead shell samples were collected between 2014 and 2016.

3.1. Study area

3.1.1 Ebro Delta, Spain.

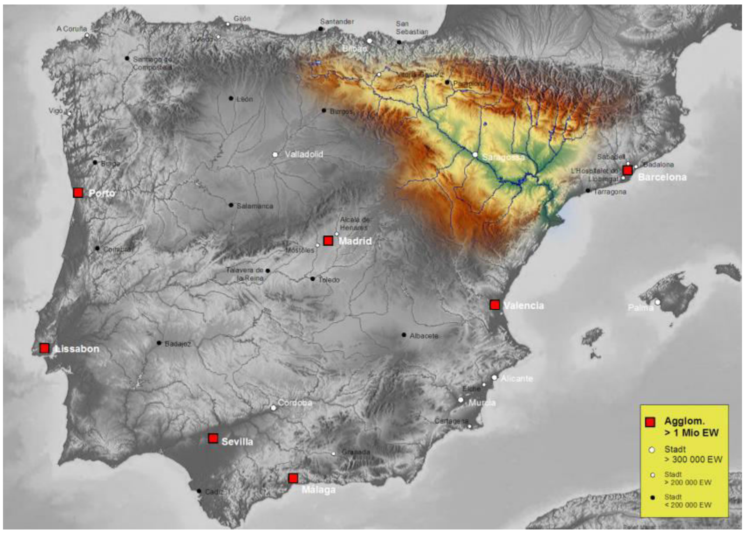

Figure 20 Ebro river course in the NE of the Spain

Figure 21 Ebro delta. In this figure are highlighted the Natural Park of Ebro delta and the two bays Fangar at the north and Les Alfaques at the south.

The Ebro River (Catalonia, NE Spain) is the largest river of the Iberian Peninsula. It originates from a natural reservoir in a forested area (elevation about 1200 m) near the town of Fontibre in Cantabria, and it flows into the Ebro Delta (Fig. 20). The river flows from the North Eastern peninsula and traverses 800 Km before terminating in the Mediterranean Sea. (Bouza-Deano et al.2008). It is a triangular shaped delta going some 20 km into the sea, with one coastal spit in the north and one in the south, these spits are close two shallow bays (Manosa et al. 2001), (Fangar Bay in the north and Alfaques Bay in the south) (Fig. 21). The Ebro Delta is a wetland area of international importance for waterbird conservation. Because of its ornithological importance, as well as for other geological, biological and cultural aspects, some of the most outstanding natural areas of the delta were included in the Ebro Delta Natural Park in October 1986. (Manosa et a.. 2001). The area is also included in the list of the Ramsar Convention and is considered as an Important Bird Area by BirdLife International. At the beginning of the 20th century, the area around the delta began to be altered due to the exploitation of resources. A large surface has been irreparably modified, and natural habitat declined from 80% to 33% with the installation of rice farms. This situation is positive because rice fields are temporary aquatic ecosystems, with periods of flooding during the summer and of drying during the winter, that is the reverse of the cycle of the natural Mediterranean wetlands. Therefore, rice fields may play an important role as substitute wetlands, especially during the drought conditions. (Fasola et al. 1996). On the other hand, the various types of pesticides to control algae, infesting dicotyledonous, crustaceans and insects may have both direct (though generally sublethal) and indirect (by lowering food availability) effects on waterbirds and Natural Park. (Fasola et al. 1996). Furthermore, rice field cultivation requires large-scale control of water inputs and outputs and so an extensive system of irrigation and drainage the canals have been constructed in the Delta. (Benito et al. 2015).

The strong anthropic presence has therefore greatly altered the aspect of this delta, which continues to offer an ideal habitat for different bird species, allows economic development from the point of view of the agricultural and aquaculture sectors, is a natural park that attracts many visitors a year, and is a very interesting area from the scientific point of view because of the different ecological features the environment has.

3.1.2 Les Alfaques Bay

Alfaques Bay (Los Alfacs Bay in Catalan language) is a large semi-closed estuarine water body located south of the Ebro River Delta NW Mediterranean, approx. 11 km^2 in length, 4 km^2 large occupied about half by a sand barrier called Banya Sandspit, connected to the land by a long sandy corridor called Trabucador on the eastern side, the bay a mean depth and maximum of 3.13 and 6.50 m. The bay is very important for the region's economy due to its fish and shellfish aquaculture, particularly oysters and mussels (Solé et al., 2009) and rice cultivation around it (Fig. 22). The bay receives fresh water from different sources, which are: the influx of the river Ebro, which, mixed with salt water in the Mediterranean enters the bay through its mouth, annual rainfall, urban waters coming from Sant Carles de la Ràpita and Poblenou delta, underground sources and irrigation channels, the latter two, however, mainly affect the ecology of this bay. These channels are fully open at 8 months per year (from April to October or November),

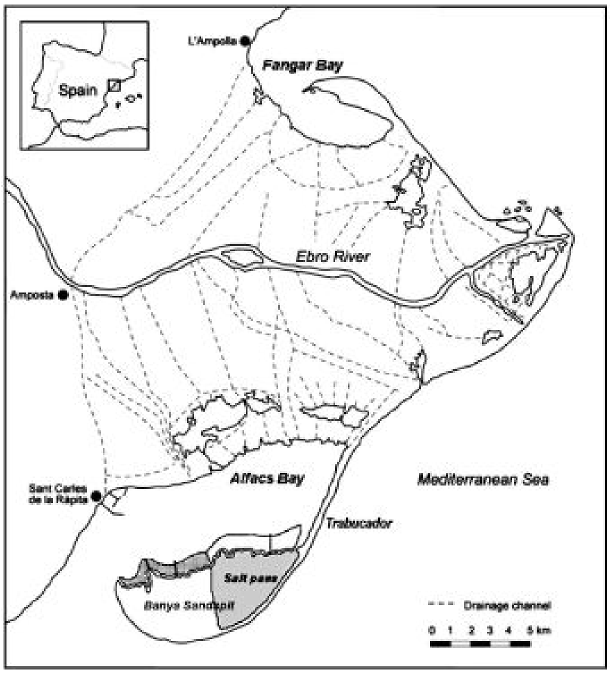

Figure 22 Ebro delta.

when rice fields are flooded, from October to mid-January the flow is reduced, and from mid-January, to April the channels are closed for maintenance (Llebot et 2014)

According to the Llebot Study of 2014, the bay waters are stratified throughout the year, and it seems to be salinity the driver of this phenomenon. This stratification persists even during the closing time of the channels, which suggests that the contribution of the underground sources is essential, while seasonal variations also indicate a major contribution by the inflows due to irrigation channels of rice fields.

As for tide hikes, they occur about every 3h, and there are 0.25 m in amplitude. Wind intensity plays an important role in this bay, in fact, surface water can be pushed to the inside of the bay, bay or in the opposite direction enhancing to the amplitude and affecting the flows towards the Mediterranean. While the deep waters currents go in the opposite direction to the superficial. So the water stratification and circulation are controlled by the influx of freshwater from the canals and from the groundwater sources on a seasonal scale, while in the short term they also influence disturbances due to strong winds blowing on the surface. The shallow submerged platform along the inner shore (<2 m) is dominated by the seagrass *Cymodocea nodosa* stains that follow a stationary equilibrium between removal and recolonization (Vidondo et al., 1997). The southern shore (Banya Sandspit) was included in the Ebro Delta Natural Park in 1986 and is part of the European Union's Natura 2000 network because it hosts both *C. nodosa* and *P. nobilis* (Ibáñez 1997), according to its status in Red List of Endangered Species for Spanish Waters (Guallart and Templado 2012). Despite this state of protection, tourists and fishing boats are free to access the area and anchored along the entire coast. There is also a ferry that works during the summer (Prado et al., 2014). The mouth of the bay is approx. 2.5 km wide and its edges are surrounded by a shallow platform of 18 km^2 (about 700 m wide) hanging gently from 0 to 1.5 m with an average depth of 0.64 m (Garcés et al. 1999) (Fig. 23). Far from the edge, the platform leads to a more pronounced slope that descends to the muddy basin at a maximum depth of 6.5 m. The northern part of the platform occupies 6 km2 and consists of silty sediments, while the eastern and southern sides, which occupy over 12 km2, are sandy (Garcés et al., 1999). The northern edge of the bay is connected to irrigation channels from rice

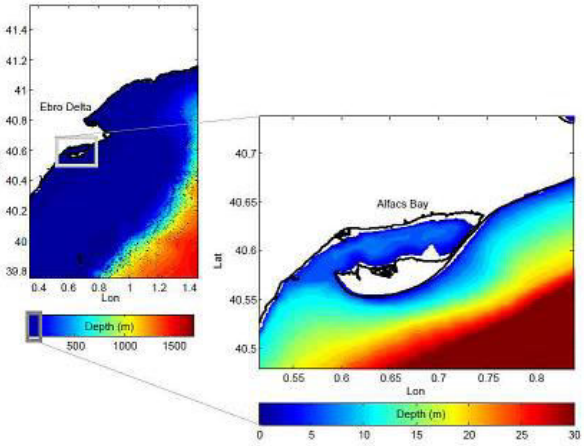

Figure 23 Les Alfaques Bay depth batimetric map.

fields that bring significant amounts of nutrients and organic matter promoting phytoplankton blooms (Delgado 1987) and fast-growth of macroalgae and freshwater decreasing the salinity in shallow waters (0 to 2 -3 m depth) to 30% and 35 ‰ (Garcés et al., 1999). The *P. nobilis* population of the bay is unusual, being present in shallow waters, less of 1m, which is already very rare and documented only in a Tunisian lagoon (see Zakhama-Sraieb et al ., 2011). Spatial distribution, too, seems to be affected depth segregation, with very few large individuals in surface and exposed areas that are increasing as depth increases. (Addis et al. 2009, Guallart and Templado 2012).

3.2 Protocol.

3.2.1 Photo.

The first step is to photograph and measure the shells. Was used a Nikon D90 Camera to take pictures of the shells (both the shells of each individual have been recorded), with a metrical scale as a reference. Furthermore, some individual with particular features, like a break or a reconstruction, were photographed in details and cataloged with a name that remembers the origin and a number, from 1 to 35. In order to confirm or deny any inconsistencies in the data at the time of the analysis, due to breaks and reconstructions of the shells (Fig. 24).

Figure 24 a,b. Alfaques10, photo pre-cut. It’s clear the break in the most posterior part of the shell.

3.2.2 Measure

We measure the following parameters:

Nº: Identifier

Htr: Total size of the specimen.

Htr (m): Total size from the most posterior to the most anterior part of the anterior adductor muscle.

A: Maximum width. Two points: 1 = maximum (although not the point of inflection) and 2 = in the point of inflection.

MAA (l): Height of the anterior adductor muscle (in points 1 dorsal and 2 ventral).
MAA (l) min: Minimum height of adductor muscle (in the center of the record).

MAA (a): Maximum width of the anterior adductor muscle..

MAPa: Distance posterior adductor muscle (most posterior part) to the most anterior part of the anterior adductor muscle.

MAPp: Distance of posterior adductor muscle to the post part. of the valve.

MAPva: Distance of posterior adductor muscle to the most anterior part of the anterior adductor muscle (of the ventral register) it does not correspond to any muscle.

MAPvp: Distance of posterior adductor muscle to the posterior part of the valve of the ventral register.

Tmap: Width of posterior adductor muscle (it would be treated as if it were a diameter).

DEM (1): Distance from the oldest posterior adductor muscle brand to the newest of anterior adductor muscle

DEM (2): Distance of the 2nd oldest mark of posterior adductor muscle the newest of anterior adductor muscle.

PUP: Distance from the first to the last clear mark of posterior adductor muscle.
H int: Internal height of the valves or internal volume (thickness).

H above: Distance from the area where the largest internal volume (H int) is measured to the most anterior part of the valve. You can subtract the difference between Htr and Htr (m), to homologate it with the other measures to the previous portion.

Pm: Migrant portion of anterior adductor muscle. From the newest brand of anterior adductor muscle to the most anterior part of the valves (measures migration and is related to erosion).

Zv: Observations on the limit between nacre and prism in the ventral area of the inner face of the valves. The minimum distance from the end of the aragonite at the end of the valve is measured.

Eje: Distance from the most anterior part of the axis by the inner side to the most anterior part of the anterior adductor muscle.

As the study is an invasive and destructive process, was organized a dimensional shell register of each specimen before proceeding with the cut. (Table 1). In order to estimate growth parameters was used a linear regression of type 2 (i.e. with both random parameters), calculated with Rstudio software. The relationship between Ht and the length of the dorsal nacre lobe was used, since several authors have shown that there is a good linear relationship between these two dimensions (García-March and Márquez-Aliaga, 2007; Moreteau and Vicente, 1982; Richardson et al. 1999), but for this analysis were used only the specimens with both dimensional measures.

3.2.2 Inclusion in resin and codification.

Figure 25 Shell imbibed in resin, with the edge delimited by plasticine, lyng on the aluminium foil.

Were selected 20 out of 35 collected shells according to their characteristics, choosing individuals representing a wide range of sizes, having both valves unbroken, not overly covered by epiphytes, and showing peculiar morphologies, e.g., obvious breaks and reconstructions, to investigate how these might have influenced the growth pattern

Then the posterior part of the shell was cut to obtain a shape that would be easier and defined to include in the resin.
The shells were placed with the internal part facing up inside a hood, on aluminum foil to protect the bottom. The shape of the shells was then delimited with plasticine to prevent the resin from dispersing and making sure that the outside of the shells remained elevated and did not touch the bottom so that the resin compound could slip under them, and they would be immersed completely (Fig 25). Then the resin fixation compound was prepared with epoxy resin and hardener epoxy resins in a ratio 2:1.

Figure 26. Group of shells immersed in resin and left under the hood for 24-48 h.

Firstly, the resin itself was deployed, then, the reagent that allows hardening the resin was added. The reagents were mixed in quantities according to the size and number of individuals to be included in the resin to avoid the waste. Following the inclusion, the resin was allowed to dry for 24 to 48 hours (Fig 26).

main line passing through the center of the PAMs, reaching the umbo of *Pinna nobilis*, divided into cross-sections. In this way, once cut, the pieces can be inserted into a slide without covering the entire surface but leaving a margin of space on the edges. (Fig. 27).

At this point each delimited piece was coded, with a criterion that includes the name of the site with the corresponding part number (the number 1 is always that of the lower end), and taking into account where the ligament is located, letter A for pieces of the ligament dorsal area (located behind it), and letter B for the pieces of the ventral ligament zone (which is separate from this).

Figure 27 Shell with guideline for the cut drawn on it

The shell ventral area, not included in resin, is encoded as "Ventral Rest". The front part coded as part 1A / 1B is defined as "Front Rest".

3.2.4 First cut.

Once all the pieces have been coded, the cutting started, starting from the transversal cross-sections, as the longitudinal line, which is very long, does not allow a precise cut. Each cross-section was then initially cut completely and then longitudinally subdivided into the two dorsal and ventral pieces, coded as A and B. All the cuts in this phase were carried out with a PROXXON MBS 240 / E ribbon saw, with NO 28186 diamond blade, equipped with a liquid cooling system, which in this case is foreseen to use fresh water (Fig. 28).

Figure 28. PROXXON MBS 240 / E ribbon saw, with NO 28186 diamond blade, equipped with a liquid cooling system

The cuts have been made slowly, in order to make them as clean as possible. The front part of the shell, coded as Front Rest, wasn't cut longitudinally, as it is not possible to detect the presence of tongues, obscured by the accretion of calcite.

3.2.5 Polishing and preparation of slices.

Once all the pieces were obtained, the ventral ones (coded with the letter B) were selected, with the exception of the individual Alfaques 17, of which the dorsals (A-coded) were selected, as the individual's ventral side was damaged. The radial part of each piece was then cleaned with sheets of sandpaper, starting with the biggest grain of 150 microns and gradually reaching the finest of 1200 microns. In this way the pieces of shell have gone from having a rough and irregular appearance, to be smooth, shiny and almost transparent. Once this level of polish is reached, the whole surface of the radial cut of each specimen was mounted in thin sections to carry out microstructural analysis, the cleaned pieces have been glued to the microscope slides with the same resin compound previously used and left to dry for a further 24 to 48 hours.

3.2.6 Second cut and second polish.

Once the resin is dry, the slit pieces on the slides were placed on rectangular metal supports and further cut with a BEUHLER ISOMET 11-1280-250 saw with a diamond blade fitted with a water-based mechanical cooling system (Fig 29). Cuts about 300 microns thick were made, obtaining a slim sheath of glued shell thanks to the resin to the microscope slide (Fig 30). During this process all slides were again cataloged with a code consisting of the individual's name, the number of the part corresponding to the slide, and the "ths1" (thin sheet 1) tag (Fig 31). Once all slides were cut and encoded, each of them was again cleaned with sandpaper, this time however, starting with a 400-micron grain to reach 1200 micron, with the aim of obtaining a smooth, glossy and transparent surface.


Figure 29 BEUHLER ISOMET 11-1280-250 saw with diamond blade fitted with a water-based mechanical cooling system


Figure 30. Moment of he cut. The piece cof shell is attached to the metal support and cutted by the saw that passed into the water to not overheat.

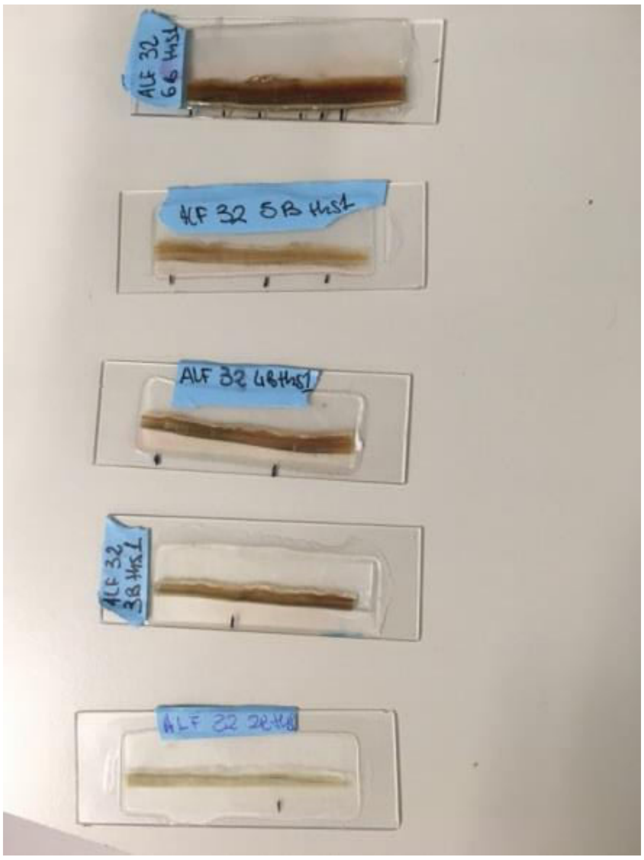

Figure 31 Slides cataloged with the thin sheet code.

3.3 Microscope analysis

3.3.1 Observation and counting of nacre tongue.

The polished surfaces of radial cuts as well as thin sheets were studied using optical microscopy (stereomicroscope) Leica MZ16. The radial cuts along the PAMS showed marks of the Inner Register (Fig. 31), some clearly visible others less, taking into account that some are well-formed, and others are still in formation.

Each of them was highlighted with a black sign on the glass (Fig. 32).

Figure 31. Inner Register.

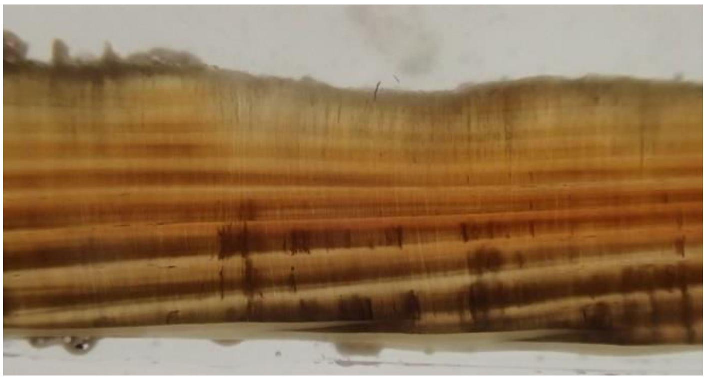

Figure 32 The nacre tongues are highlighted with a sign on the glass, with a black permanent marker.

3.3.2 Distance between brands

The distance between two successive brands was measured, starting from the back of the shell, with a precision gauge, considering the thickness of the cut between two slides, 0.4 mm. In addition, the distance between the oldest observed mark and the tip of the shell was calculated by measuring, in the absence of marks, the length of slides obtained from the most anterior pieces of the shell, and adding the length of the front rest. In this way the total distance between the newest nacre tongue and the tip of the shell was obtained.

There is a good linear relationship between shell length and the youngest leading edge of the dorsal nacre lobe (Richardson et al. 1999). Therefore, by fitting an equation between these 2 dimensions, with the distance between the brands, it is possible to extrapolate the corresponding shell lengths when each PAMS was deposited. (Hendricks et al 2012). The values measured were inserted into an Excel CSV file, to prepare the dataset to inserte in the software Rstudio, starting with the specimens that had more data, that act as a reference for the insertion of the others. The values included in the CSV file were analyzed, to calculate the cumulative sum of the measurements, and convert them in cm, with the follow equation:

$$Y = ((x * b) + c)/10$$

Where Y is the corresponding shell lengths when each brand was formed, x is cumulative sum of the distance between the brands, and the two values b and c are the slope and the intercept of the regression line that dashed the dispersion graph of our data, respectively.

3.3.3 Calcite width

The last step of the protocol is to measure the width of the calcite layer present in the thin sheet of each *Pinna nobilis*. This measurement was carried out with the LAS Version 4.4.0 [Build: 454] software, which allowed to work on the slide directly through the microscope connected to the computer. Three calcite widths were recorded at the front, center, and rear of the three older tongue drawers respectively. An average of these three measures was then made for each tongue. Because calcite tends to obscure nacre tongues that are formed in the early years of the animal, and therefore are no longer visible, by measuring the breadth of this layer, we could estimate the missing records. The three older references measured were plotted, the three allineated averages obtained allow to estimate the relation between widths in mm and the age of the individual. By reporting the data in the chart, with a common origin, the differences in the calcite width are highlighted. Then were calculated and added the numbers of missing years based on calcite increments, that are too wide to be considered the first year. The procedure was repeated for the shells that were too wide to be considered second, and so on. Keeping a conservative approach so that no extra years are added or subtracted, all records must always fall into the previsional model, where the minimum and maximum are determined by the younger individuals.

3.4 Non-Linear Model Mixed Effect

Knowing Lmax and length/age, it is possible to estimate the growth rate of the population and of each individual of the population using von Bertalanffy's growth function Lt = Lmax (1 -- $e^{-k(t-t0)}$). Where t is length corresponding to each age. The von Bertalanffy growth model (von Bertalanffy 1938) is the most commonly applied among longitudinal models and, although other models have been used, it seems to be the most suitable for growth of *P. nobilis* (Hendricks et al., 2012). In this equation the parameters K (growth constant, asymptotic attainment speed) and t0 (initial size) were calculated with the Rstudio software. A Non-Linear Model Mixed Effect (NLME) is then applied to the data, which uses the exponential function to obtain the growth curve and, is defined as mixed effect becouse it contains fixed and random factors, in this case K and t0 were set as fixed while the random value was Lmax.

3.5 Size and age classes subdivision

Once the corresponding size and age were obtained, the work was continued with the analysis of the structure of the studied dead shell population. The 20 individuals were divided into size classes. The class interval of 10 cm was based on the study by Abbiati et al. (1992) which showed the average annual growth rate of coral colonies, in this study, the use of class interval of 10 cm size has been resumed to represent the absolute frequency of individuals for each size class. Eight age classes were identified and represented by histograms using the Office package program Excel2007. The frequency of each size and age class were included, trying to represent in the better way the structure of the dead shell population.

4. Results

4.1 Shell dimensional register

Table 1 Shells dimensional register

		Htr	Htr(m)	A1	A2	Peso	MAA(l) 1	MAA(l) 2	MAA(l) min	MAA(a)	MAPa	MAPp	MAPva	MAPvp	tMAP	DEM(1)	DEM(2)	PUP	H int	H anterior	Pm	Zv	Eje	Observaciones
Número	**Valva**	cm	cm	cm	cm	g	mm	mm	mm	mm	cm	cm	cm	cm	mm	cm	cm	cm	cm	cm	mm	mm	mm	
Alfaques 1	**R**	40.6	40.0		18.9	193.4	24.9	24.9	15.5	12.4	22.2	17.8	25.0	15.8	29.3	17.0	19.2	1.9	3.4	29.3	29.4	4.1	50.5	
Alfaques 1	**L**	41.0	40.0		18.5	200.2	22.4	24.5	21.7	12.6	21.6	19.0	24.8	15.6	26.7	17.0	18.7	1.8	4.1	27.9	37.2	4.3	43.6	
Alfaques 2	**R**	50.0	47.7	17.2	16.2	430.6	30.3	34.1	28.9	21.8									3.6	33.4	65.6	4.0		much epibionts
Alfaques 2	**L**	48.9	47.2	17.4	15.5	417.4	30.7	32.6	29.1	21.6	28.3	18.8	32.5	16.4	40.4	19.5	21.7	5.6	3.9	28.8	57.4	5.7	69.6	
Alfaques 3	**R**	50.0	47.5		17.2	346.2	29.6	28.3	24.3	15.3	23.8	24.4	30.0	18.9	26.5	15.5	21.4	4.7	3.8	31.0	52.0	6.7	49.7	depression outside
Alfaques 3	**L**	49.2	47.2		17.4	335.0	27.7	26.2	25.1	15.4	23.5	24.5	30.6	18.5	31.6	15.6	21.0	4.4	4.2	30.2	48.8	4.8	49.4	depression outside
Alfaques 4	**R**	51.5	48.3		17.2	309.9	27.9	26.7	25.4	16.3	24.9	24.9	29.5	21.5	35.7		20.9		3.7	30.0	56.8	5.5	55.0	much epibionts
Alfaques 4	**L**	50.5	48.7		17.3	301.5	26.8	27.8	24.2	16.8	24.6	24.0	34.5	17.3	34.1		21.9		4.3	29.5	54.9	5.3	51.2	
Alfaques 5	**R**	49.7	47.1		17.1	294.8	30.0	26.7	23.6	18.1	25.8	21.7	32.4	16.7	31.9	18.5	20.6	4.7	3.7	27.7	53.5	5.3	92.7	
Alfaques 5	**L**	47.8	44.3	17.4	17.1	300.6	28.1	28.8	26.7	16.1	25.4	21.7	32.5	16.0	29.4	18.5	20.5	4.0	3.5	27.2	49.5	5.2	84.2	
Alfaques 6	**R**	51.5	50.0		18.6	441.2	33.8	30.2	25.7	17.2	26.0	24.0	30.0	22.0	34.7	18.7	20.7	3.6	3.4	30.0	48.2	6.1	82.4	
Alfaques 6	**L**	51.8	49.7		18.9	387.0	30.7	31.1	29.1	17.9	25.8	24.6	29.0	21.4	34.3	19.0	20.9	3.7	3.5	27.4	54.1	5.3	70.5	
Alfaques 7	**R**	58.7	56.2		18.7	981.2	19.4	21.9	16.9	25.8	30.0	22.0	36.7	19.9	48.7	16.0	18.1	12.0	4.3	34.7	82.5	5.6	41.8	reconstruction upside
Alfaques 7	**L**	52.1	57.0		17.9	952.6	50.5	52.8	50.3	27.7	33.2	23.5	37.5	19.6	45.2	16.2	22.6	11.5	5.1	41.0	105.2	3.9	74.9	
Alfaques 8	**R**	46.6	44.4	20.0	18.3	355.7	28.5	27.4	25.0	15.7									3.9	29.4	48.5	7.3	63.4	Broken downside, with reconstruction inside, much epibionts
Alfaques 8	**L**	46.5	45.0		19.9	348.8	24.2	24.8	23.0	13.4									4.3	28.8	45.7	6.5	67.9	Broken downside, much epibionts
Alfaques 9	**R**	53.5	50.6		17.6	333.8	25.9	23.6	24.0	17.3	26.0	22.5	31.1	18.3	28.4	15.5	18.0	7.4	3.5	29.9	56.1	5.5	59.8	
Alfaques 9	**L**	51.5	50.5		17.0	335.0	24.0	24.6	23.7	16.1	26.0	24.3	32.5	20.4	30.1	17.9	20.5	4.2	3.5	27.5	39.4	4.7	57.2	
Alfaques 10	**R**	42.4	40.3		20.0	392.7	29.1	30.1	28.8	20.6	26.9	16.8	32.9	8.0	36.3	18.4	20.9	5.7	3.9	23.0	57.9	5.2	51.3	Broken downside
Alfaques 10	**L**	54.6	51.9		20.5	495.4	30.0	29.4	28.1	18.6	26.6	21.2	32.2	21.9	37.8	21.3	24.0	5.2	4.5	27.3	60.6	8.2	49.3	Broken downside
Alfaques 11	**R**	49.1	46.9		18.2	344.8	32.6	34.6	29.9	17.5									3.3	27.6	58.4	5.4	58.7	Broken downside, much epibionts
Alfaques 11	**L**	49.2	46.6		18.5	358.6	33.8	35.8	30.7	16.1									3.5	30.4	59.7	6.6	52.7	much epibionts
Alfaques 12	**R**	59.4	57.0	20.9	20.5	514.1	33.1	34.4	29.3	21.2	28.6	28.5	32.5	25.5	36.5	20.0	22.5	5.2	5.1	29.0	62.4	6.6	62.2	broken dorsal side
Alfaques 12	**L**	58.2	56.7	21.0	20.9	519.4	33.5	36.1	31.2	20.3	28.2	28.0	32.6	25.5	35.7	19.8	21.9	5.3	5.0	25.0	52.8	5.9	63.9	broken dorsal side (deformada)
Alfaques 13	**R**	49.5	47.0		16.3	351.4	29.0	29.4	25.7	17.3	25.5	19.9			28.9				3.9	30.4	58.6	3.5	82.5	much epibionts
Alfaques 13	**L**	50.2	46.7		16.4	369.3	30.4	29.8	25.6	18.2					27.9	16.1	19.1	4.8	3.5	22.0	63.0	2.3	108.8	much epibionts
Alfaques 14	**R**	43.0	42.0	17.8	17.5	273.1	24.8	24.2	23.8	14.1	23.1	19.0	24.2	18.6	29.7	18.6	20.6	2.1	3.2	19.6	34.2	5.8	50.1	
Alfaques 14	**L**	43.3	42.1		17.5	281.2	23.3	23.7	21.7	14.0	23.2	19.0	24.3	18.5	32.1	18.7	21.0	2.4	3.1	19.0	37.1	6.1	66.3	
Alfaques 15	**R**	55.7	52.7		19.0	609.7	37.2	37.1	35.4	21.2									3.6	30.3	68.6	5.3	79.8	much epibionts
Alfaques 15	**L**	56.0	53.4		19.0	631.2	37.6	37.1	35.8	21.5	30.5	22.4			39.0				3.7	27.4	67.1	6.5		much epibionts
Alfaques 16	**R**	56.5	52.2		18.0	463.9	26.9	28.2	26.3	19.1	27.8	25.6	29.5	25.0	30.4	19.4	21.8	5.7	4.2	27.4	60.6	6.2	98.8	Broken upside
Alfaques 16	**L**	55.7	52.9		17.9	484.9	27.6	30.0	28.3	19.3	27.0	25.6	29.1	24.8	35.3	19.1	21.5	5.2	4.0	26.2	59.3	5.6	87.4	
Alfaques 17	**R**	43.1	41.9		17.2	222.1	21.8	22.2	19.4	15.3	22.5	19.3	24.3	17.7	29.8	17.1	20.3	3.4	2.4	22.8	39.6	5.7	55.5	
Alfaques 17	**L**	42.8	41.9		17.5	236.3	23.0	23.9	20.3	14.5	22.5	19.2	24.2	18.0	31.1	19.1	22.5	3.4	3.2	24.5	36.3	6.4	53.7	piece of the other valva makes false the h int
Alfaques 18	**R**	60.5	57.3		18.5	577.3	30.1	30.9	28.6	20.1	28.6	28.8	36.1	22.6	34.5	19.1	21.2	6.2	4.2	32.9	63.9	5.6	54.3	
Alfaques 18	**L**	59.4	57.2		18.5	584.6	32.6	33.3	30.2	20.5	28.0	29.2	35.8	23.7	35.2	19.2	21.6	9.3	4.5	33.6	57.7	6.4	51.2	
Alfaques 19	**R**	59.4	56.7		19.5	473.8	28.7	28.3	24.5	21.4	28.5	27.6	36.0	22.8	32.1	19.7	22.4	6.1	4.2	37.3	60.0	4.3	55.8	
Alfaques 19	**L**	59.8	56.3		19	437.9	26.4	29.3	24.9	21.3	28.7	27.6	36.7	22.5	34.0	19.9	22.2	6.3	3.9	34.6	64.6	5.6	53.2	BROKEN UPSIDE
Alfaques 20	**R**	52.5	49.5		16.1	306.3	30.1	32.1	27.8	15.9	26.7	22.9	32.2	19.5	35.3	20.4	24.0	3.1	3.4	29.2	57.8	5.4	99.0	
Alfaques 20	**L**	51.7	49.8		16.4	310.3	30.5	32.7	27.8	17.4	27.0	22.7	30.9	21.0	33.9	20.4	23.8	3.1	3.4	29.1	56.5	4.3	95.6	
Alfaques 21	**R**	62.2	58.5		18.8	542.3	33.4	37.6	30.7	24.7	31.4	27.4	36.7	24.3	43.2	21.7	24.0	6.2	4.0	37.5	72.2	5.0	71.9	
Alfaques 21	**L**	59	59	18.8		543.1	30.9	32.7	28.6	25.0	31.4	27.8	35.4	25.8	42.7	21.7	24.7	7.0	4.5	31.9	48.5	6.5	71.8	BROKEN INFLEXION POINT
Alfaques 22	**R**	56.7	54.4		14	416.7	35.5	35.8	30.1	20.8	28.4	26.3	34.5	22.0	29.9	16.0	20.0	8.4	4.3	21.0	62.0	4.0	71.9	reconstruction
Alfaques 22	**L**	55.4	53.9		14.3	410.4	33.8	33.4	30.9	21.6	21.7	26.1	36.4	19.5	27.3	16.0	19.9	8.5	4.3	24.0	55.2	5.9	90.8	
Alfaques 23	**R**	55.3	53.5		17.7	45505						23.5							3.6	27.0			77.5	much epibionts
Alfaques 23	**L**	55.5	53.8		18.2	498.7													4.0	30.2				MUCH EPIBIONTES
Alfaques 24	**R**	38.1	36.3		14	221.3	23.0	23.0	20.5	14.2	20.0	16.5	23.1	14.7	29.3	14.0	18.0	4.0	4.0	20.9	38.2	5.3	49.5	piece of the other valva makes false the h int
Alfaques 24	**L**	38.5	36.7		14	207.4	20.5	24.2	21.0	13.3	20.1	16.6	24.0	14.0	29.2	13.0	14.0	5.0	4.0	22.0	45.7	5.8	39.5	
Alfaques 25	**R**	57.5	55.3		16.8	553					31.4	23.5	33.6	23.3	36.4			5.7	4.4	30.2		5.1		broken
Alfaques 25	**L**	57.7	53.7		16.1	505.4	37.4	35.8	33.3	23.2	31.3	22.6	34.3	21.5	36.2	22.1	24.2	5.6	4.1	35.6	74.6	6.1		
Alfaques 26	**R**	49	46.9	17.5	14.7	297.5					24.2	22.6	27.4	21.3	30.1			4.0	3.5	29.0		3.3	55.0	BROKEN DOWNSIDE, impossible to see the musculo anterior
Alfaques 26	**L**	49.8	47.8		17.4	307.8						24.0		20.9	30.7				3.6	22.7		4.5		impossible to see the musculo anterior
Alfaques 27	**R**	44.9	43.2		19.3	297.1	24.7	25.1	22.0	13.6	23.1	21.0							4.0	27.6	44.5	6.1	47.4	BROKEN DOWNSIDE, much epibionts
Alfaques 27	**L**	45	43		19	302.2	23.4	25.7	22.3	13.0									4.0	27.5	48.2	3.8	44.2	BROKEN DOWNSIDE
Alfaques 28	**R**	51	48.9		18	425	31.1	29.5	26.2	17.5	28.9	22.4	31.1	20.0	32.4	21.1	22.8	3.8	3.9	34.3	48.0	6.5	73.8	BROKEN DOWNSIDE
Alfaques 28	**L**	52.1	49		17.2	422.2	30.5	29.7	27.1	16.0	28.0	21.4	30.5	20.0	30.5	20.9	22.9	3.7	4.4	34.0	58.2	5.7	65.2	much epibionts make false h int
Alfaques 29	**R**	53	49.2		18	386.3	25.8	23.5	20.4	18.1	26.3	22.2	31.6	17.8	32.0				3.8	31.4	63.2	4.3	58.0	BROKEN DOWNSIDE
Alfaques 29	**L**	54	50.7		18.2	376.1	23.9	25.8	22.7	17.2	27.0	24.1	31.1	20.0	31.0				4.0	30.2	58.4	4.5	50.3	recontruction downside
Alfaques 30	**R**	53.6	51.6		20	517.3	32.0	34.5	30.8	23.4	29.0	22.0	32.0	20.5	40.6	19.9	21.8	6.1	3.7	27.1	54.3	5.3	70.4	BROKEN DOWNSIDE
Alfaques 30	**L**	55.3	51.7		20	516.4	32.5	34.9	31.3	22.7	28.4	21.8	33.4	18.7	39.8	19.4	21.7	5.6	3.5	28.5	72.9	5.4	50.2	BROKEN DOWNSIDE
Alfaques 31	**R**	51.7	50		19	391.8	27.4	25.6	23.7	14.5									3.5	29.6	48.0	4.5	64.6	much epibionts
Alfaques 31	**L**	50.3	49.5		19	380.3	27.8	25.7	24.0	13.1									3.5	28.5	32.9	5.3	66.6	much epibionts
Alfaques 32	**R**	60.5	58.4	16		744.7	37.3	36.0	32.7	22.4	32.4	26.0	39.0	21.0	45.6	20.1	22.5	8.8	4.1	36.3	58.3	3.7	60.0	BROKEN INFLEXION POINT
Alfaques 32	**L**	59.8	57.6	16		739.8	39.9	38.3	34.5	22.6	32.2	26.2	39.6	21.0	41.1	19.9	22.3	9.0	4.2	28.1	58.3	2.5	64.6	BROKEN INFLEXION POINT
Alfaques 33	**L**	46.5	44		16.5	310.2	23.9	27.9	23.4	15.7	24.3	20.5	25.5	20.0	31.0	15.6	19.0	8.8	3.7	30.9	52.7	2.8	44.5	
Alfaques 34	**L**	45	42.8		15.2	240.8	26.1	27.4	24.9	18.3	25.1	15.6	26.7	17.0	37.7	19.4	22.6	3.2	3.2	21.6	47.5	5.9	57.3	Broken downside
Alfaques 35	**R**	33.7	33		17.7	198.3	23.2	20.5	18.1	10.3	20.3	13.7	21.4	12.1	24.3	16.1			4.1	27.2	33.4	4.6	48.1	Broken in half
Alfaques 35	**L**	34.5	33.5	17.9	17.6	214.5	23.2	21.4	19.8	11.2	20.2	13.4	21.4	12.2	22.8	17.0			3.2	16.9	33.4	4.4	54.0	Broken in half

The data for the two Ht and MAPa variables were plotted into a dispersion graph, which places MAPa as an independent variable and Ht as a dependent variable, so it is possible to verify the trend of the data. If there is a linear relationship or if there are abnormal values.

4.2 Linear Regression type 2.

The Total size/MAP distribution fits a linear model (Fig. 33). The only exception is the specimen Alfaques 22, showing an unusual shape of the shell. This specimen was removed form the data set for the following analyses.

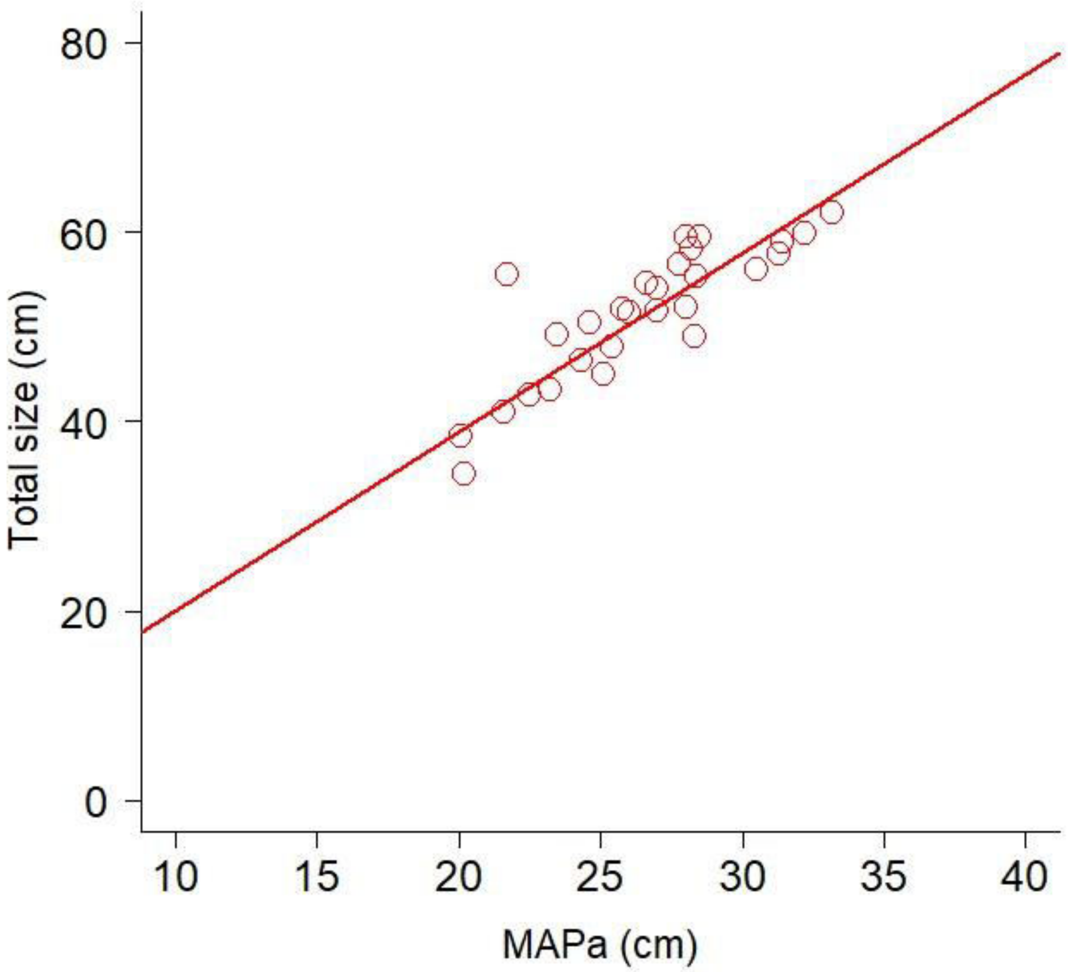

Figure 33 Linear regression type 2 graphic, with an outlier, Alfaques 22.

The relationship between Total size and MAP fits well with a linear model across all individuals (Fig. 34).

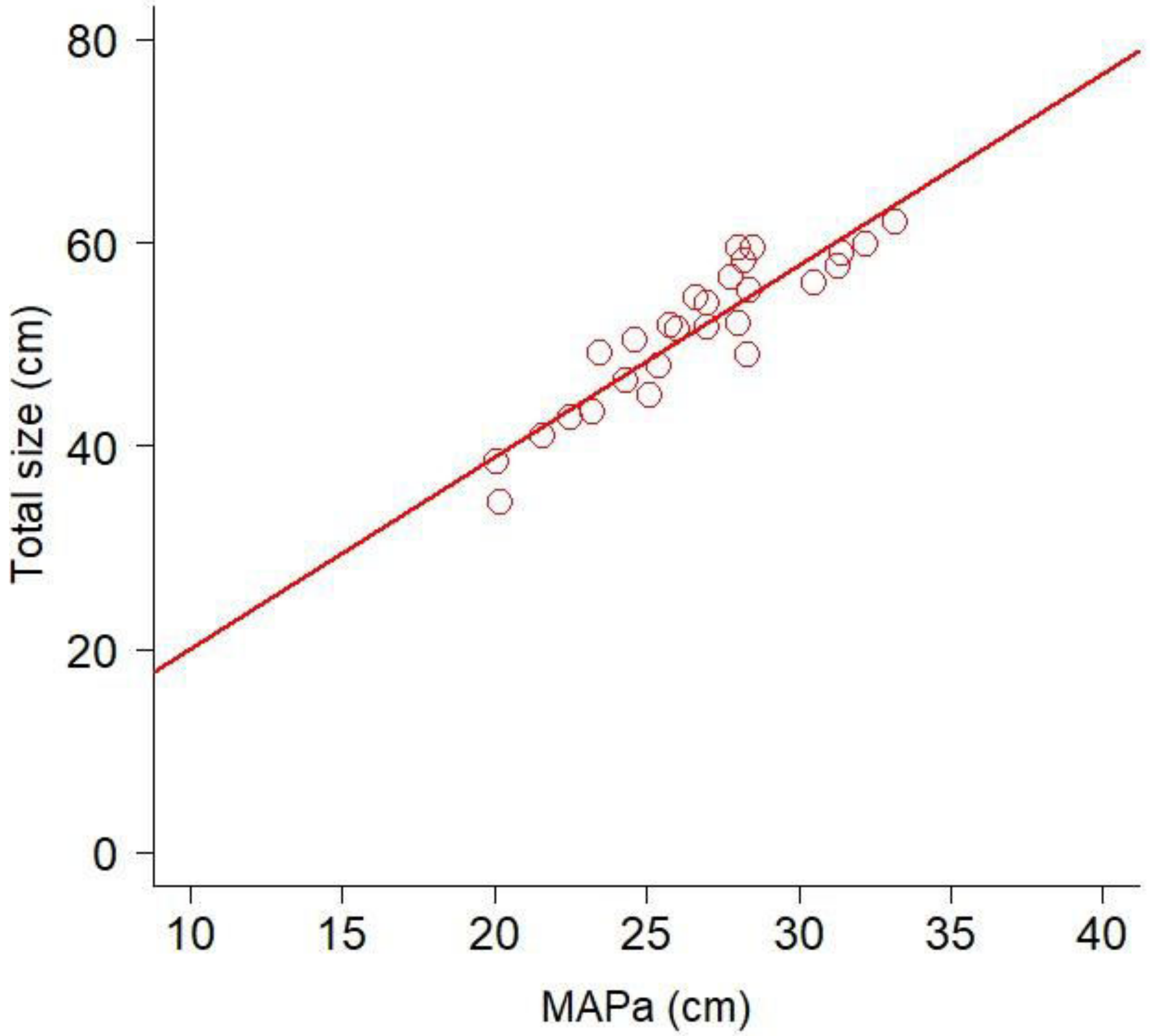

Figure 34 The model without the outlier.

The regression equation was calculated with the Rstudio software:

$$Ht = 1.8834 * MAPa + 1.2413$$

The linear regression was significant by the Student's test, t = 11. 376 (p-value = 2.24e-11) for the angular coefficient, and F of Fischer, F = 129.4 (p-value: 2.238e-11). Moreover, the R^2 coefficient of determination, was equal to 0.8381, which means that the regression explains 83.8% of the variability of the data**.**

4.3 Distance between brands

From the calculation of the distance between the brands, and based on the linear relationship between the distance between each brand and the umbo of the shell, with the maximum shell size, the size of each individual for each year from the first year of life was calculated (Table 2). Reading the table it's possible to see that the size at the first year of the different specimens ranges between 21 and 36 cm. From previous studies, results that is overestimated.

Table 2 Temporary age-size table, without considering the unregistered year.

AGE	CODE	CODE	CODE	CODE	CODE	CODE	CODE	CODE	CODE	CODE	CODE	CODE	CODE	CODE	CODE	CODE	CODE	CODE	CODE	CODE
	Alf2	Alf5	Alf6	Alf7	Alf10	Alf12	Alf13	Alf14	Alf16	Alf17	Alf18	Alf19	Alf20	Alf21	Alf23	Alf26	Alf28	Alf30	Alf31	Alf32
1	36.85043	27.20742	36.71859	31.25673	29.58051	30.2962	23.7608	22.27291	30.33387	29.26033	29.18499	40.40252	36.21761	27.68957	31.07028	23.65721	26.77612	21.61937	36.53967	22.8869
2	44.17686	32.01009	38.07464	38.86567	38.48899	39.11051	35.92756	33.47914	38.90334	36.8316	39.05401	47.39182	47.90222	39.30073	40.81499	33.84076	36.4681	34.53573	42.51758	29.83665
3	48.33917	37.92397	44.72304	45.00555	45.40107	46.39927	43.23516	41.37059	45.51407	43.19749	45.89075	52.19072	54.24551	47.74778	46.26931	39.45329	43.54968	43.46681	44.8982	36.81088
4	52.35081	38.43249	49.1302	50.2414	49.86472	50.91943	48.1885	45.74008	50.0154		50.59925	56.33797		53.28686	51.04562	43.85479	49.82141	50.82526	47.93612	42.29346
5	54.62973	41.21992	52.0683	54.49789	52.87816	54.91224	52.0118		53.46202		54.74273	59.12352		57.64317	54.07601	46.72133	53.34713	55.38685		46.64788
6		43.74367		58.96155	54.9499	56.73913			55.96694		56.70147			60.37598	56.07994		57.06685	59.0576		51.16615
7		45.28806		61.5418											56.78245			61.91095		53.96112
8				64.70592																55.92362
9				66.41981																57.49249
10				68.71756																59.20262
11				70.24311																61.17077
12				71.52382																62.15579
13				71.69333																63.07866

The age-size relationship emerging from this table is provisional, and not exhaustive, considering that the first year of life is not registered (Richardson et al 1999), and that the most anterior portion of the calcite is usually lost in the adult individuals shell, and therefore 1 year should be added (Garcia and Aliaga 2007). This underestimation of the age was corrected by adding one year to each individual (Table 3).

Table 3 Size-age table with the addition of the first unregistered year highlighted in yellow.

AGE	CODE	CODE	CODE	CODE	CODE	CODE	CODE	CODE	CODE	CODE	CODE	CODE	CODE	CODE	CODE	CODE	CODE	CODE	CODE	CODE
	Alf2	Alf5	Alf6	Alf7	Alf10	Alf12	Alf13	Alf14	Alf16	Alf17	Alf18	Alf19	Alf20	Alf21	Alf23	Alf26	Alf28	Alf30	Alf31	Alf32
1																				
2	36.9	27.2	36.7	31.3	29.6	30.3	23.8	22.3	30.3	29.3	29.2	40.4	36.2	27.7	31.1	23.7	26.8	21.6	36.5	22.9
3	44.2	32.0	38.1	38.9	38.5	39.1	35.9	33.5	38.9	36.8	39.1	47.4	47.9	39.3	40.8	33.8	36.5	34.5	42.5	29.8
4	48.3	37.9	44.7	45.0	45.4	46.4	43.2	41.4	45.5	43.2	45.9	52.2	54.2	47.7	46.3	39.5	43.5	43.5	44.9	36.8
5	52.4	38.4	49.1	50.2	49.9	50.9	48.2	45.7	50.0		50.6	56.3		53.3	51.0	43.9	49.8	50.8	47.9	42.3
6	54.6	41.2	52.1	54.5	52.9	54.9	52.0		53.5		54.7	59.1		57.6	54.1	46.7	53.3	55.4		46.6
7		43.7		59.0	54.9	56.7			56.0		56.7			60.4	56.1		57.1	59.1		51.2
8		45.3		61.5											56.8			61.9		54.0
9				64.7																55.9
10				66.4																57.5
11				68.7																59.2
12				70.2																61.2
13				71.5																62.2
14				71.7																63.1

4.4 Estimation of missing records

In this study, the estimation of the missing records required 3 steps. In the first, all the records were charted to the one called "initial position" (Fig 35), with a common origin. In this step, the difference between the calcite thickness of Alfaques 5, Alfaques 13, Alfaques 14, Alfaques 26 and Alfaques 30 compare to the others shells was evident. These five shells have a smaller thickness, and considering that the width of calcite at each annual increment is a function of the number of years deposited (i.e. age) because calcite stops growing when the nacre covers it on the inner side of the shell (García-March and Márquez-Aliaga, 2007), were considered the younger individuals.

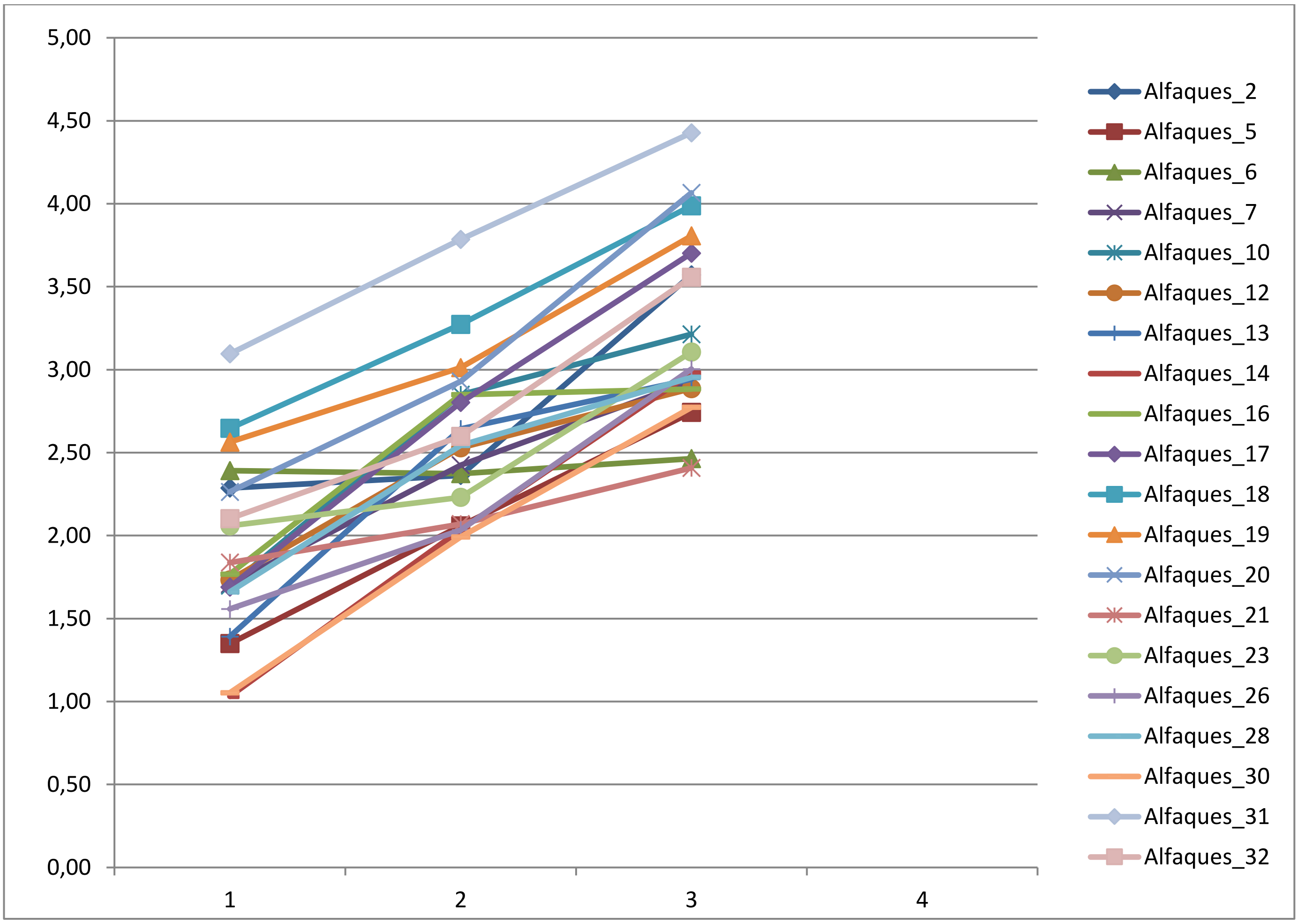

Figure 35 Initial position.

In the next step, was added one year to all individuals except the five younger defined above (Fig. 36).

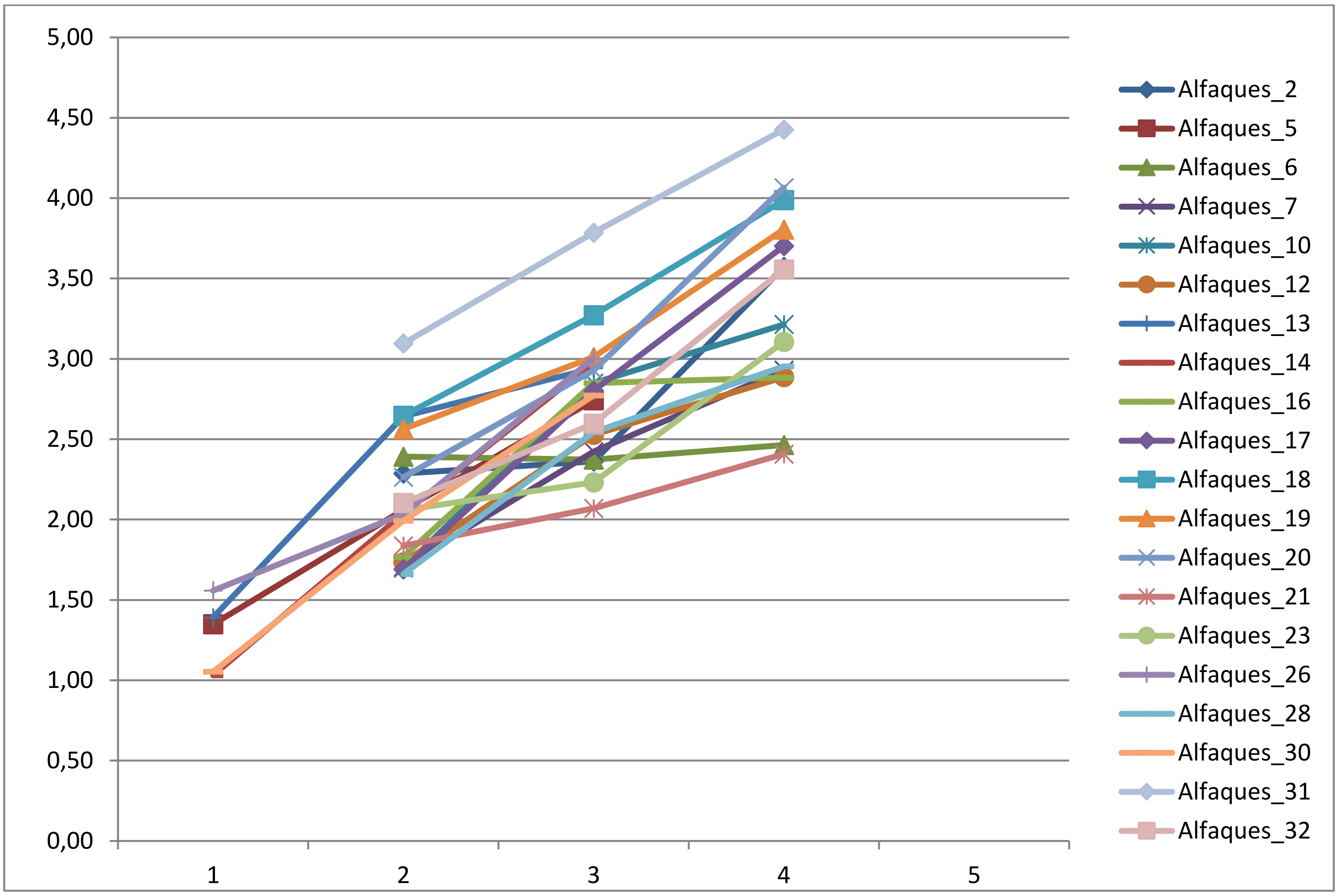

Figure 36 Step 2.

In Figure 36, discrepancies in the thickness of the calcite in four specimens, Alfaques 18, Alfaques 19, Alfaques 20, Alfaques 31, are quite evident. In particular, Alfaques 31 differs greatly from all other individuals, having a layer of calcite very thick. In the last step (Fig 37), another year was added to individuals 18,19 and 20 and two years to individual 31. Getting a chart that fits the expected pattern of each individual.

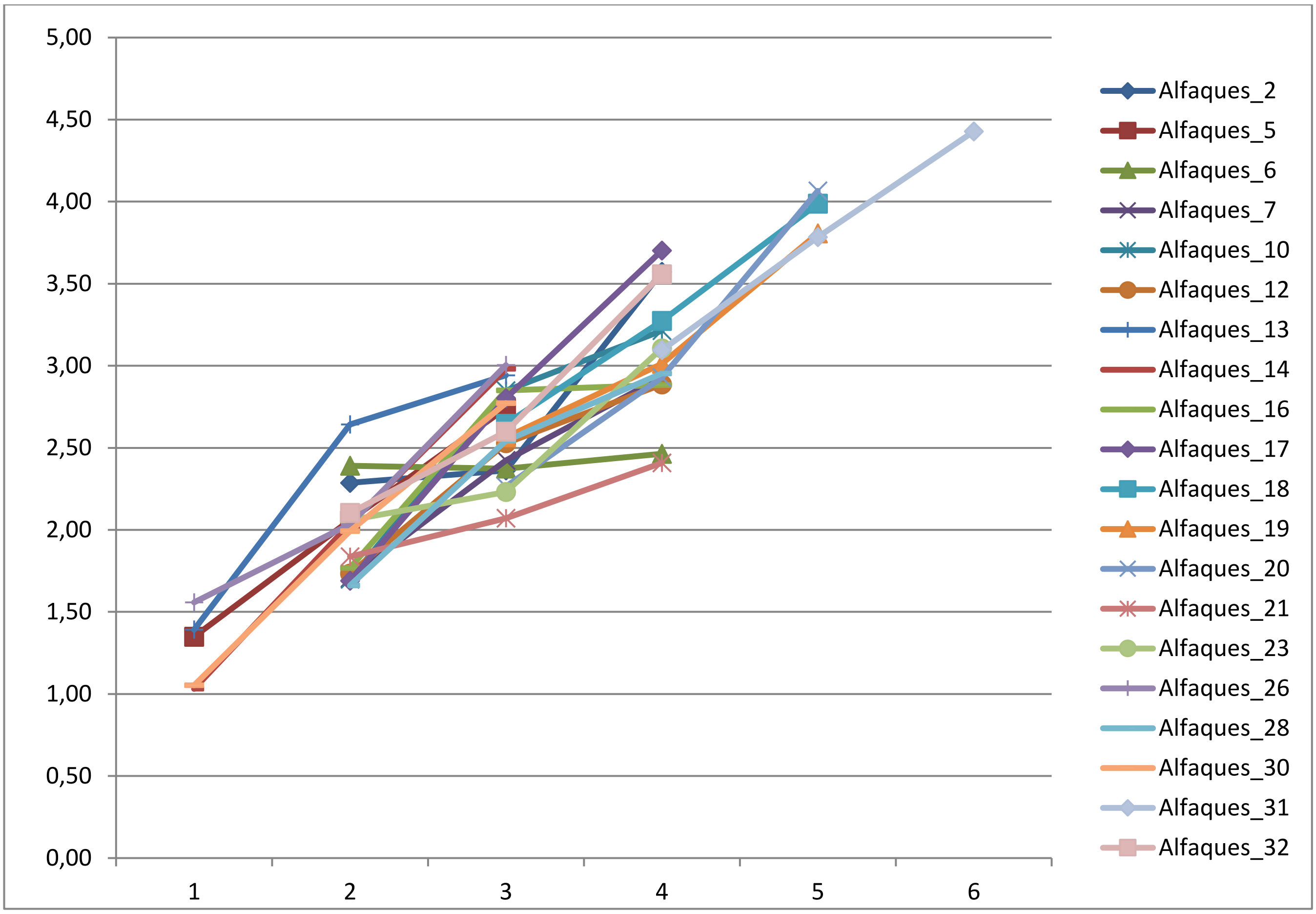

Figure 37 Step 3.

Following this process of recalculating the age based on the thickness of the calcitic layer overlapping the nacre layer, the corrected age of all shell has been reported (Table 4).

Table 4 Size-age table with the correction made by the missing records.

AGE	CODE	CODE	CODE	CODE	CODE	CODE	CODE	CODE	CODE	CODE	CODE	CODE	CODE	CODE	CODE	CODE	CODE	CODE	CODE	CODE
	Alf2	Alf5	Alf6	Alf7	Alf10	Alf12	Alf13	Alf14	Alf16	Alf17	Alf18	Alf19	Alf20	Alf21	Alf23	Alf26	Alf28	Alf30	Alf31	Alf32
1																				
2		27.2						22.3								23.7		21.6		
3	36.9	32.0	36.7	31.3	29.6	30.3	23.8	33.5	30.3	29.3				27.7	31.1	33.8	26.8	34.5		22.9
4	44.2	37.9	38.1	38.9	38.5	39.1	35.9	41.4	38.9	36.8	29.2	40.4	36.2	39.3	40.8	39.5	36.5	43.5		29.8
5	48.3	38.4	44.7	45.0	45.4	46.4	43.2	45.7	45.5	43.2	39.1	47.4	47.9	47.7	46.3	43.9	43.5	50.8	36.5	36.8
6	52.4	41.2	49.1	50.2	49.9	50.9	48.2		50.0		45.9	52.2	54.2	53.3	51.0	46.7	49.8	55.4	42.5	42.3
7	54.6	43.7	52.1	54.5	52.9	54.9	52.0		53.5		50.6	56.3		57.6	54.1		53.3	59.1	44.9	46.6
8		45.3		59.0	54.9	56.7			56.0		54.7	59.1		60.4	56.1		57.1	61.9	47.9	51.2
9				61.5							56.7				56.8					54.0
10				64.7																55.9
11				66.4																57.5
12				68.7																59.2
13				70.2																61.2
14				71.5																62.2
15				71.7																63.1

In this way, we get a corrected size/age relationship, allowing us to associate each size with a given year of life for each individual. The oldest specimens among those analyzed are Alfaques 7 and Alfaques 32, both with 15 years of age.

4.5 Non-Linear model mixed effect

The NLME based on the Von Bertalanffy equation, allowed the calculation of the growth curve of Les Alfaques bay population (Fig 38). The growth rate is not particularly high, and the curve reaches a plateau at about 10 years of age. This result is unexpected, considering the depth at which the shells were collected. The curve, in fact, reaches and exceeds slightly 70 cm, for individuals supposed to be about 15 years old, so more or less half of their lifespan.

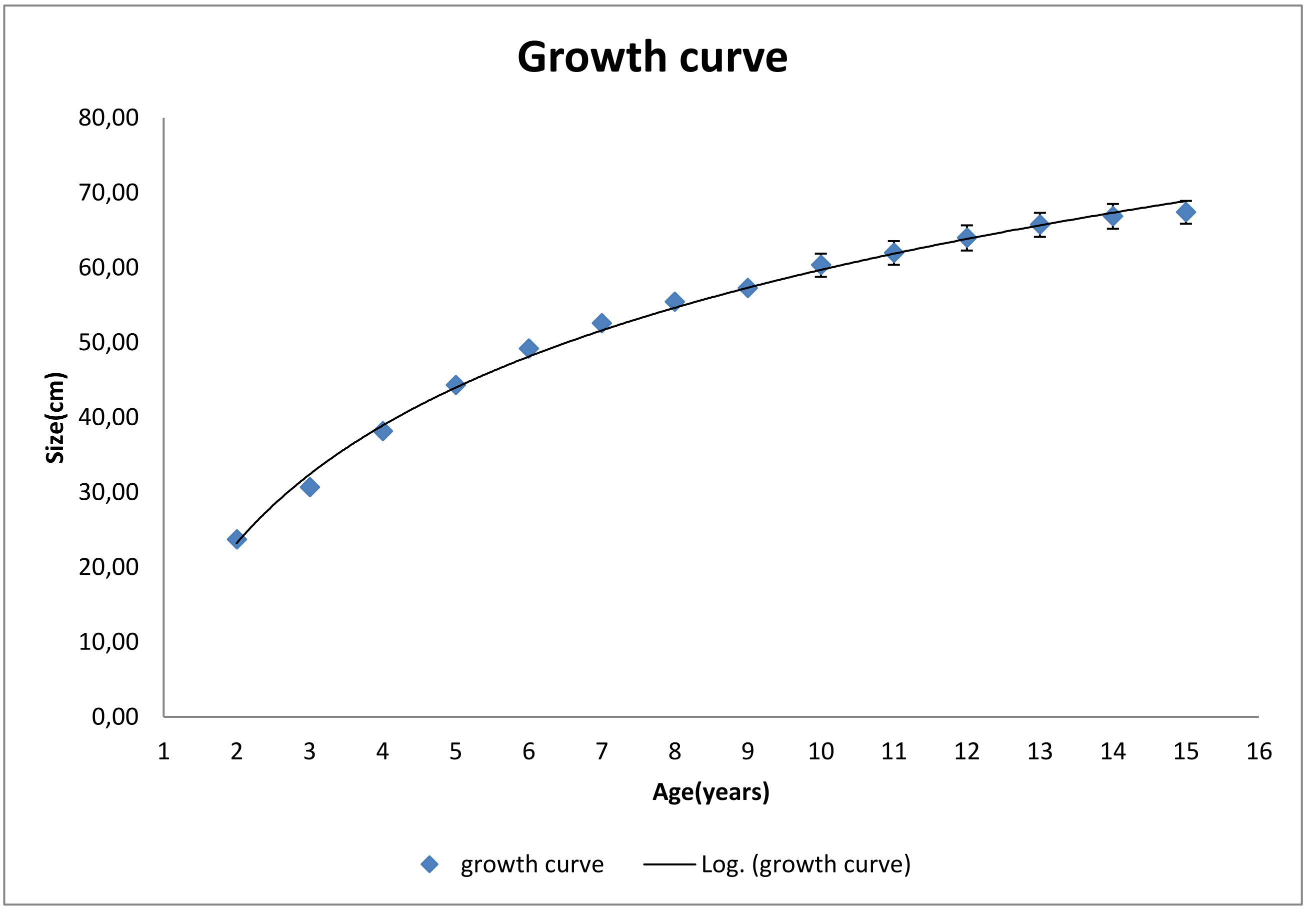

Figure 38 Growth curve of Les Alfaques Bay population.

Using the same model, the Los Alfaques population growth rate (line blue) was compared with the growth rate estimated for each specimen (pink id line) (Fig19). In this way, it’s possible to highlight individual variability within the population. It is possible to notice how some specimens fit perfectly the model, while others deviate from it (Fig. 39)

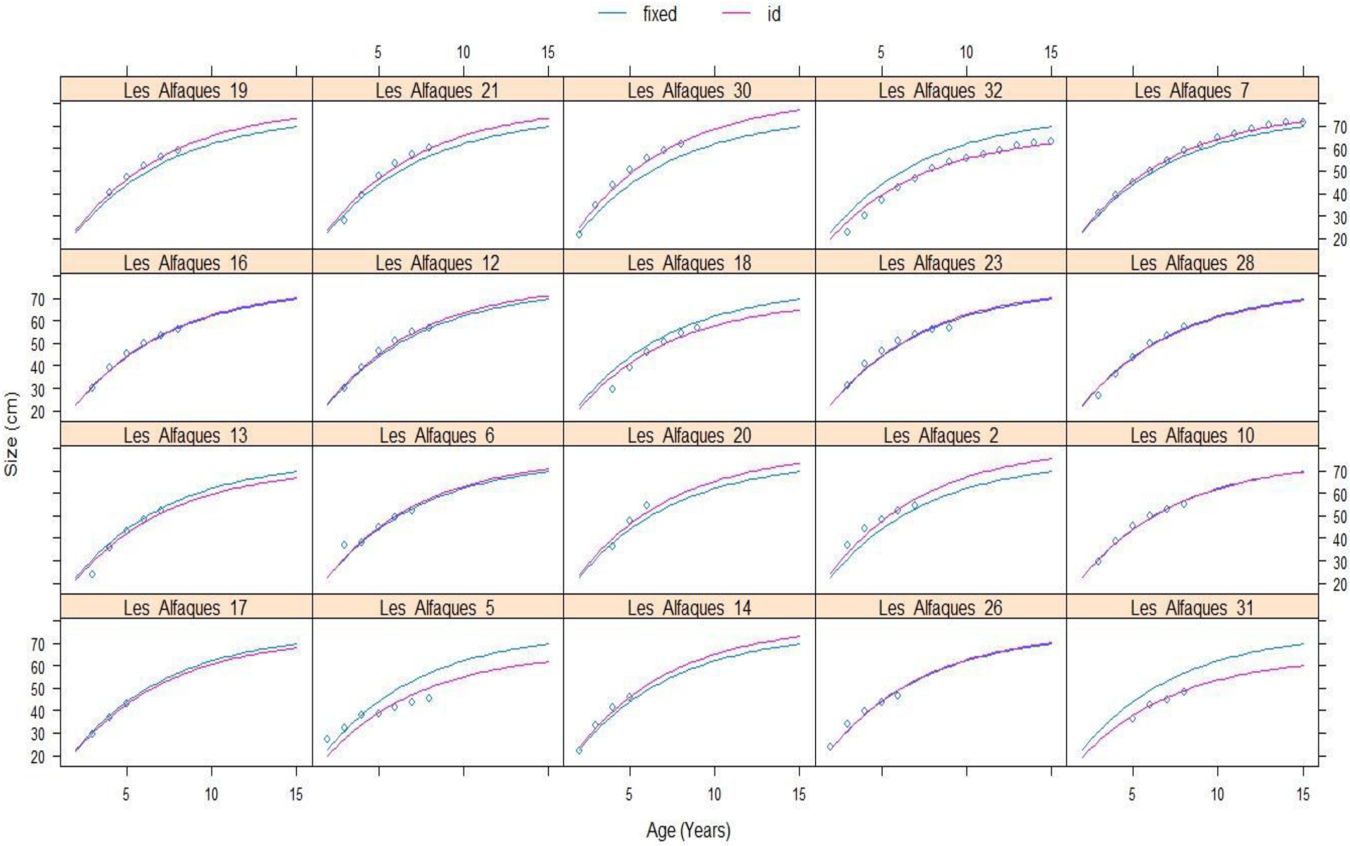

Figure 39 Comparison between individual growth curve and population growth curve.

Using the Von Bertalanffy equation, a predictive model or population growth was produced (Fig. 40). Based on the data collected, and thanks to the Von Bertalanffy equation, it was possible to project on the graph the potential growth that individuals of this population could experience under the conditions that generated the measured growth rate. From the equation, there is a maximum potential size (Lmax = 75cm) and at this size, the growth curve reaches its plateau

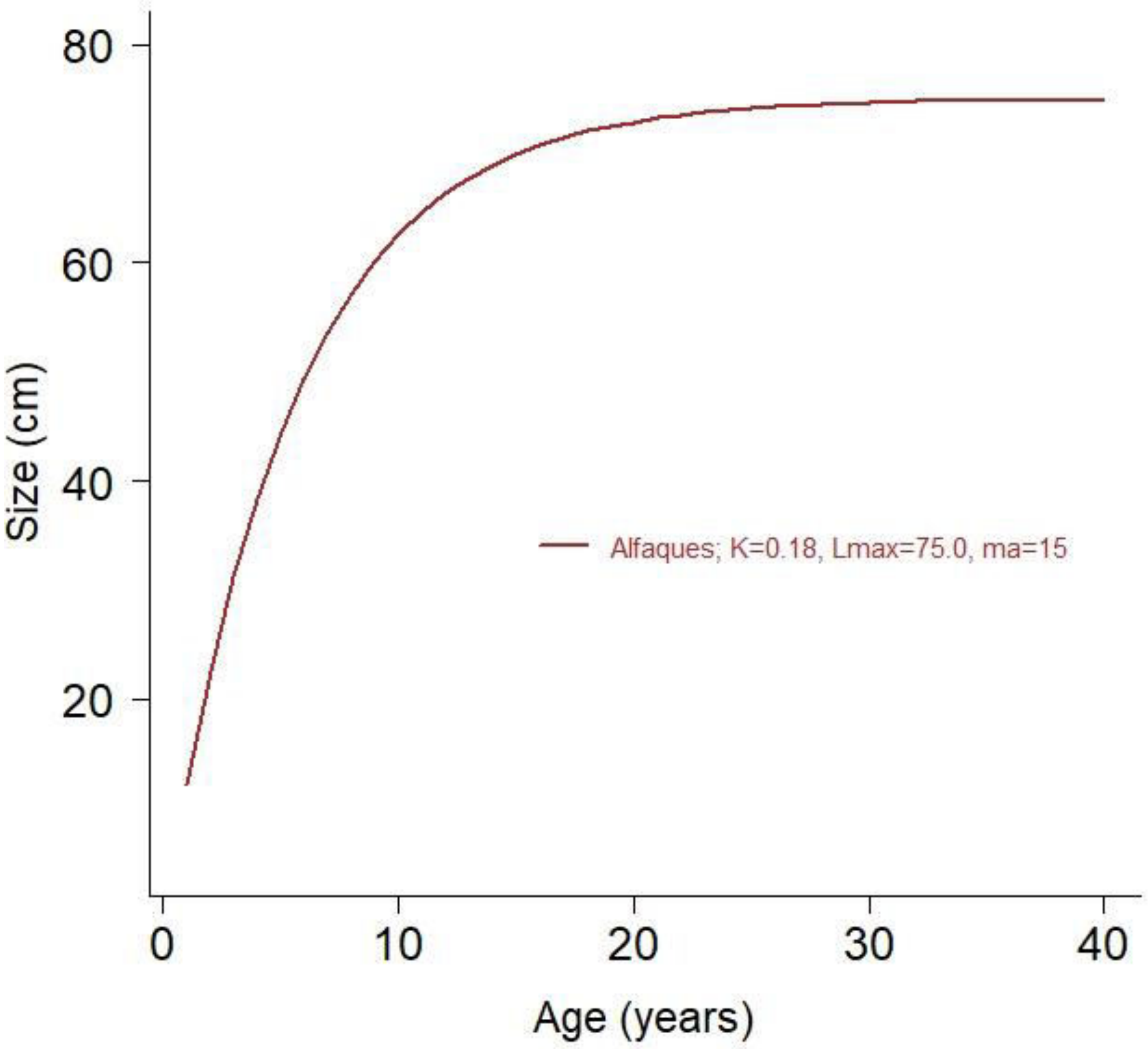

Figure 10 Predictive growth curve of Les Alfaques Bay population.

4.6 Size and age classes subdivision

From the matrix on the size classes obtained from the collected samples, and using the size class ranges suggested by (Abbiati et al. 1992) a size class distribution with 10cm class intervals was made. The predominant size is ranging between 50-60 cm (Fig. 41). We notice that the smaller size classes (0-40 cm) are missing. This feature of the sample could be related to the sampling conservative approach, where only dead shells have been collected.

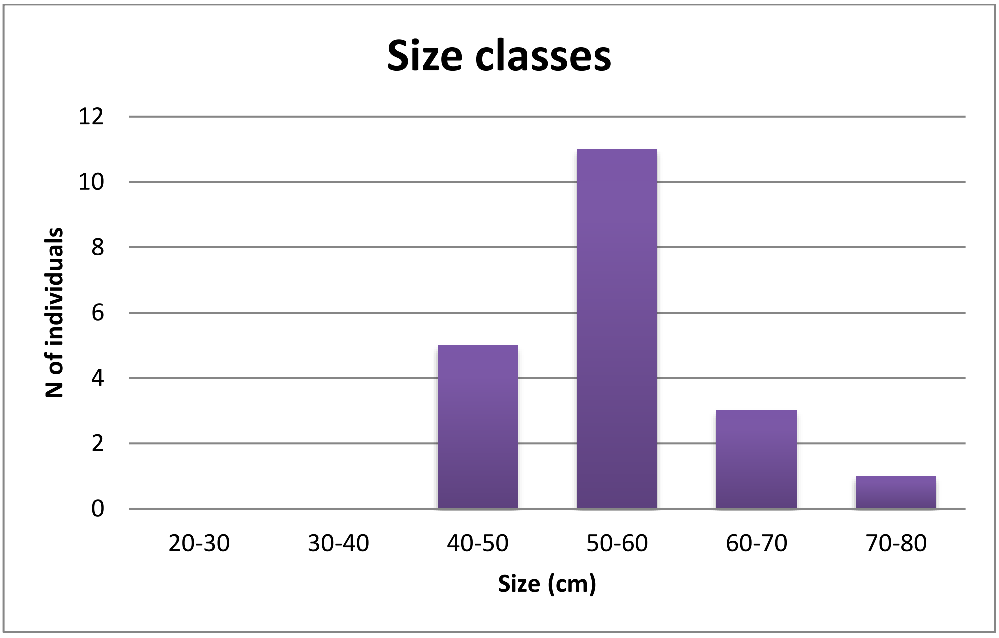

Figure 41 Size composition of the Los Alfaques Bay population.

Most of them are concentrated in the age group of 8-9 years.

Figure 42 Age composition of Los Alfaques Bay population.

If the collected specimens are analyzed on terms of age structure (Fig 42) it’s possible to observe that the youngest individuals are about 4 years old and it is made by adult individuals (Fig.42), There is also a gap between the 9 years and 14 years old individuals, which is not easy to explain.

5. Discussion

5.1 Linear regression

The relationship between of the total length of the shell and the position of the posterior muscle position follows linear regression. The linear regression is significant for the intercept and the slope of the straight line. All the specimens follow this trend except for Alfaques 22. The shell of this specimen has a different shape compare to most specimens (Fig. 43, 44).

Figure 43,44 Specimen Alfaques 22 with a particular shell shape.

The shell is very elongated and with a strong curvature that starts from the center of the valve, where it is possible to observe that is has been damaged in the past. At this point there was a major deposition of calcite and of nacre during growth, probably due to reconstruction. The unusual shape is likely due to the asymmetrical growth after the injury.

5.2 Distance between brands

In the samples analyzed in this study the shells were between 43 and 71 cm in length, and between 4 and 14 years old, and young specimens were absent. Several authors believe that estimating the age of *Pinna nobilis* from the external register involves errors, as many old PAMS could be obscured by nacre in the anterior part of the old specimens and that deposition of new records could be overlapped, confounding the age counts from PAMS (Garcìa-March and Aliaga 2007). By studying the internal register, it was possible to identify and mark nacre tongues that were not visible from the PAMS, and by the cumulative sum of the distance between the brands, it was possible to estimate the size of the shell at the time when each brand was deposited. The estimated age of the specimens was found to be more likely than the one derived only from the external register. It is also known from previous studies that during the first months after metamorphosis, and during the first few years, the organisms grow primarily along the major axis. Only when they reach ca. 20 cm in length shells growth is primarily in width (Hendricks et al., 2012). In the second year there was a slowdown in growth that occurred concurrently with the appearance of the "first" ring of the adductor-muscle scar. Any estimates of the growth rates of the pinnids should take in account the fact that the first-year ring is missing. The first ring was masked by nacre deposited on the inner shell surface (Richardson et al., 2004). In large and very old shells, even the second ring may be masked by deposition of shell material over the muscle scar (Richardson et al. 1999). Thus the age-related relationship obtained by the cumulative sum of brand distance has been updated by adding the first missing year, getting a range of ages between 5 and 15 years

5.3 Estimation of missing years

From the studies of Garcia-March and Aliaga (2007) and Garcia-March (2011), it turns out that the age of *Pinna nobilis* is often underestimated because of the absence of external and internal evidences of the first years of life of the specimen. To minimize errors due to this absence, and to provide more accurate size-age estimation, the thickness of the calcite layer was studied. The calcite increments of the 3 older brands were used in all individuals, to avoid any differences due to deposition of calcite at later stages, or the abrasion of the calcitic layer in the front part. Calcite deposition is an annual process, so individuals with lower average calcite thickness were considered younger and used as a reference in the process. This is a critical assumption and it may bias the age estimations. However, this approach has been used in García-March (2011) to study a population of *Pinna nobilis* in the bay of Moraira, and in Nebot-Colomer et al. (2016) to investigate the population structure and growth rate of *Pinna rudis* in a marine protected area in the Western Mediterranean. Based on the thickness values used as a reference, the growth range was defined by comparing them with older individual, which had a significantly higher calcite thickness, and was 15 years old.

The trend following the plotted lines is increasing (Fig 37), reflecting the increase in the average thickness of the calcite layer over time. The specimen Alfaques 6 shows a different pattern, the line seems to be parallel to the x-axis, with a slight increase in the last stroke. From the length/age relationship shown in Table 4, it is noted that the specimen Alfaques 6 between the second and third year grew only 1.4 mm. The next year it grew 6.6 mm. Also, as noted in the picture, the two brands (the oldest and the next one) are very close together (Fig.45). It could be assumed that this second brand is a "fake brand", i.e. formed after less than a year. This can happen when the individual stops its growth due to damage, and invests most energy to rebuild the broken part, and then continue the normal growth process. This causes the formation of nacre tongue similar to the annual ones, but formed in a shorter time. In this case, the nacre tongue was not considered to be a false mark because it has all the features of an annual brand

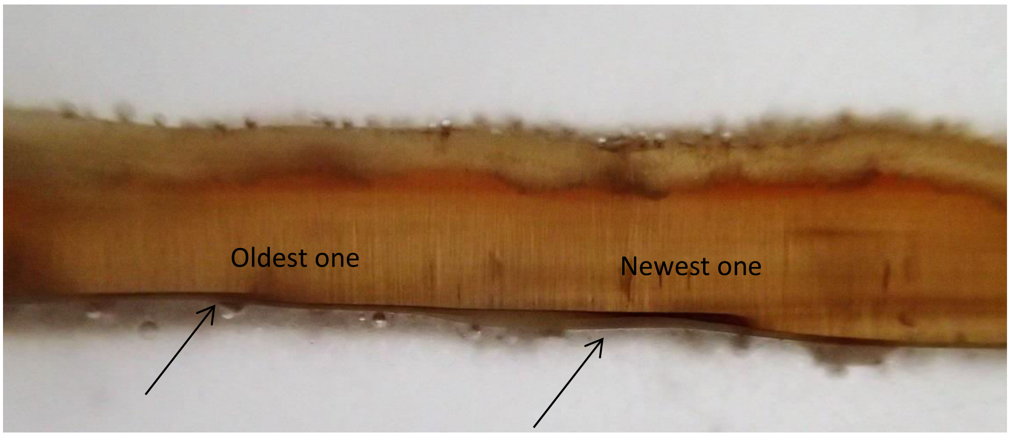

Figure 45 Two nacre tongues really close together in specimen Alfaques6.

The number of years calculated using the calcite increment estimates was added to all individuals getting the Table 4 that better represents the size-age relationship of each specimen. Damaged individuals may produce a greater quantity of calcite than normal, or calcite may be abraded over time, so the thickness of the calcite can be variable and lead to an overestimates or underestimates of the missing records and consequently of the age of the animal. A shell having thicker calcite for the same age may lead to an overestimation of age by 1 year (Garcìa-March et al. 2011). For example, the individual 30 measured about 61 cm in length but age was estimated to be 8 years, while the specimen 32 measures 63 cm to and age estimation was16 years. Alfaques 31 reaches about 48 cm at the same age of 8 years as Alfaques 30. It is possible that Alfaques 30 had a slower calcification rate. It is also possible that this individual grew very rapidly in the first part of his life, there is a gap of about 10 cm between the third and fourth year of age, and about 8 cm between the fourth and fifth and then proceed normally (see Table 4). During this rapid ontogenesis it's possible that some nacre tongues have been obscured, and so it has not been possible to register them It could be an example of underestimation of the individual's age, which could be one or more years older, just like the Alfaques 21 individual, who had a similar pattern (see Table 4). Not to force the model further, and to avoid mistakes due to excess of indirect estimates, this trend was maintained since it appeared to be the most conservative and representative for the available data.

Determining the precise age of this species is very difficult, internal variability within organisms is very strong and reconstructing the early years of life is a delicate step in the protocol. Although it is susceptible to errors, this new method permits an accurate and more complete counting of records and their crossdating using calcite width (Garcìa-March et al 2011), and seems to be the only one able to consider the years that are not recorded in the growth marks. At this stage, it is appropriate to add the minimum number of years allowing a reasonable correspondence with the thickness of calcite found. The underestimation of the years, corresponding to the initial size, is a compromise to be accepted to avoid overestimating the total age of the individual.

5.4 Non-Linear Model Mixed Effect

The growth curve of this population, based on the analysis of 20 individuals, has a rather readable trend with minimum standard errors. From this curve emerges that the measure reached by the population at the age of 15 is just under 70 cm. Though they have been found at low depths, these individuals are of considerable size, and show a rather consistent growth trend. This growth trend is also found in other studies such as in Siletic et al. (2003) conducted in Mljet National Park in Croatia, where *Pinna nobilis* reaches a height above 65 cm in 15 years.

During ontogeny, growth is characterized by changes in proportion and size, called allometric growth. Such a change in growth trajectory could be a useful source of information about the life story of the pen shell or a fast-ecological change (Hendricks et al. 2012). The growth curve is therefore a useful tool for studying the ecology of *Pinna nobilis* and the habitat where ontogenesis has occurred. The growth rates of bivalves may be associated with food availability, temperature, upwelling intensity, sediment type and hydrodynamics (Newell & Hidu 1982, Steffani & Branch 2003, Ackerman & Nishizaki 2004, Philips 2005). Several studies have shown that the growth rate of shellfish will change in response to changes in temperature and salinity (Paynter & DiMichele 1990, Paynter & Burrison 1991, Kennedy, Newell & Eble 1996, Shumway 1996, Dekshenieks, Hofmann, Klinck & Powell 2000). Specifically, for *P. nobilis*, severe sediment disturbances and high hydrodynamic stress have been suggested as causes for reduced growth (Garcìa-March, Perez-

Rojas et al., 2007). Thanks to the growth curve of a population it is possible to hypothesize the causes that generated the observed pattern and eventually deepen the study. Furthermore, since *Pinna nobilis*, is a species protected by the European Habitats Directive (Directive 92/43 / EEC) and the Barcelona Convention, many studies on the growth of this bivalve were carried out in the Mediterranean (Raboui et al 2007,2011, Kozul et al., 2012, Garcìa-March et al., 2002,2007,2011, Hendricks et al., 2012). The growth curve of this study is the first constructed for the bay of Les Alfaques, and with the aim to monitor this species, it is proposed as baseline for future studies on the ecological characteristics of the habitat that may have affected the growth rate and the size of the analyzed specimens.

This study can provide a useful reference mark for comparison with populations from other sites, as well as other regions and, may reveal if changes in growth pattern are specific for the species or related to the regional features and linked to local changes (Hendricks et al. 2012). The proposed methodology reduces the costs and working time in the field, while respecting the current rules on handling live animals. In addition, the described growth curve that constitutes the baseline for the Les Alfaques bay, can allow for monitoring of this population over time, as carried out by Silec et al (2003), which describes an increase in the total population size of the Mljet National Park from 1998 to 2000.

The growth model based on the modified Von Bertalanffy equation was used to simulate the growth rate of the population of Les Alfaques bay, since this is the most studied and commonly applied model among all the length-age models (Raboui et al., 2011). Secondly, according to García-March (2011), author of the new age-determination methodology used in this work, among all methods tested to fit the Von Bertalanffy growth model, LA data from internal records better fit while using non-linear mixed effects. Moreover, the estimation of missing records using the calcite width, seems to be the most appropriate. The equation obtained with this method is very similar to that previously calculated from in situ measurements (Garcia-March 2011). According to the model, this population could reach a plateau with a total shell length of about 75 cm. It would be interesting to deepen the studies on the bay of Les Alfaques, in order to increase the data to support this model. It is known that growth parameters of VBGM are quite inaccurate when estimated based on a dataset without having specimens of large sizes close to the asymptotic length (Raboui et al 2007), Therefore, it is important to have an appropriate dataset for the application of this method. The variability among populations is to be considered, in fact some *P. nobilis* populations seem to reach an asymptote in their growth at quite small size and early in life, while others grow much larger and become more than double in size. For these reasons it is better to compare the curves of the growth models within the range of sizes encountered in each dataset, rather than to compare the estimated parameters (Raboui et al 2007).

5.5 Size and age classes subdivision

Size and age classes show a homogeneous pattern. The majority of individuals are between 50-60 cm in size, and between 8-9 years old. These values correspond to the age-related values also reported in other studies on the same topic (see Richardson et al., 1999). The population has a shell of rather high dimensions considering the depth at which the drawing took place. Many authors in many different areas have reported a depth-related size segregation in *P. nobilis* (Zavodnik 1967; Moreteau and Vicente 1982; Vicente 1990; Vicente and Moreteau 1991; Katsanevakis 2006a, 2007; García-March et al. 2007a, 2007b). The observed pattern was common: smaller individuals occurred more often in shallower waters, while larger individuals were more abundant in deeper water, and were usually absent from the shallow waters (Katsanevakis 2007). The hypothesis made by some researchers to explain this size segregation was that recruitment was favored in shallower areas and then young individuals could move deeper during ontogeny (Zavodnik 1967; Moreteau and Vicente 1982; Vicente and Moreteau 1990). García-March et al. (2007a) questioned this hypothesis and pointed out that there was no solid proof of the potential of young fan mussels to migrate deeper in any of the former studies. The high number of filaments and the attachment strategy of *P. nobilis* imply that the animals stay sessile reinforcing continuously and, by all means possible, the fixation to the substrate. Furthermore, the entire byssus needs up to 6 months for its regeneration (Cerruti, 1938, 1939; Mihailinovic, 1955). It is unlikely that an animal would shed the filaments voluntarily to move a few meters, leaving itself vulnerable to predators and to hydrodynamics stress for such a long period of time (Garcìa-March, 2005).

This distribution is more likely related to the hydrodynamism, as it is given a wave height, individuals of shallower levels are subjected to higher drag forces than those located at deeper ones (Grarcìa-March et al 2006). The effects of hydrodynamics on size, shape and distribution of benthic organisms are still not completely understood. More commonly, *Pinna nobilis* depth distributions peak at ranges from 3 to 15 m (García-March et al. 2006, Garcia-March and Kersting 2006, Katsanevakis 2007, Coppa et al. 2013) and may be explained by the need to minimize exposure to wave action, as also evidenced by increasing valve sizes at greater depths and shell orientations coincident with the exposure that minimizes hydrodynamic effects (García-March et al. 2007a,b). In the bay of Les Alfaques, wave protection is provided by the sand bar of the Banya Sandspit, which acts as a hydrodynamic barrier. The bay also houses a *Cymodocea nodosa* meadow, which is an ideal habitat for *P. nobilis*. It is therefore assumed that being a sheltered and protected habitat, this bay allowed the development of unusually large individuals compared to the standards reported in other studies for shallow populations. It is possible that in this bay mortality affects larger individuals, higher the 50-60 cm in size. Considering that in this species natural mortality was strikingly size dependent and *P. nobilis* suffered high natural mortality during the first year of life, mortality by natural causes quickly diminished as the fan mussels grow in size (Katsanevakis 2007). We can hypothesize that the samples analyzed in this study died all because of non-natural causes. In the bay of Les Alfaques, there is a very strong anthropic impact. Although the Ebro Delta area is a natural park, and especially the Banya Sandspit area is inserted into the Natura 2000 network, approximately half of this sandbar is occupied by a salt factory with extensive salt pans, and recreational and fishing boats are free to access to the area and anchor along the entire shoreline. In addition, there is also a ferry operating regularly between the port in Sant Carles de la Ràpita and a snack bar located close to the mouth of the bay that attracts high numbers of tourists to the area during the summer period (Prado et al. 2014). It’s therefore possible hypothesize that when they reach the size of 50-60 cm, in such a shallow area, these individuals are killed by accidents due mainly to the anchorage, or the propellers of the boats in that area. This hypothesis is supported by the numerous break-up scars found in most shells of this population.

6. References

Abbiati, M., Buffoni, G., Caforio, G., Di Cola, G., & Santangelo, G. (1992). Harvesting, predation and competition effects on a red coral population. *Netherlands Journal of Sea Research*, *30*, 219-228. 1

Ackerman, J. D., & Nishizaki, M. T. (2004). The effect of velocity on the suspension feeding and growth of the marine mussels Mytilus trossulus and M. californianus: implications for niche separation. *Journal of Marine Systems*, *49*(1), 195-207.

Addis, P., Secci, M., Brundu, G., Manunza, A., Corrias, S., & Cau, A. (2009). Density, size structure, shell orientation and epibiontic colonization of the fan mussel Pinna nobilis L. 1758 (Mollusca: Bivalvia) in three contrasting habitats in an estuarine area of Sardinia (W Mediterranean). *Scientia Marina*, *73*(1), 143-152.

Basso, L., Vázquez-Luis, M., García-March, J. R., Deudero, S., Alvarez, E., Vicente, N., ... & Hendriks, I. E. (2015). Chapter Three-The Pen Shell, Pinna nobilis: A Review of Population Status and Recommended Research Priorities in the Mediterranean Sea. *Advances in marine biology*, *71*, 109-160.

Benito, X., Trobajo, R., Ibáñez, C., Cearreta, A., & Brunet, M. (2015). Benthic foraminifera as indicators of habitat change in anthropogenically impacted coastal wetlands of the Ebro Delta (NE Iberian Peninsula). *Marine pollution bulletin*, *101*(1), 163-173.

Bouza-Deaño, R., Ternero-Rodríguez, M., & Fernández-Espinosa, A. J. (2008). Trend study and assessment of surface water quality in the Ebro River (Spain). *Journal of Hydrology*, *361*(3), 227-239.

Carter, J. G., & Clark, G. R. (1985). Classification and phylogenetic significance of molluscan shell microstructure. *Studies in Geology, Notes for a Short Course*, *13*, 50-71.

Cerruti, A. (1938). *Primi esperimenti di allevamento della Pinna" Pinna nobilis L." nel Mar Piccolo di Taranto*. Tipografia Terme.

COLOMER, E. N., Vazquez-Luis, M., Garcia-March, J. R., & Deudero, S. (2016). Population Structure and Growth of the Threatened Pen Shell, Pinna rudis (Linnaeus, 1758) in a Western Mediterranean Marine Protected Area. *Mediterranean Marine Science*, *17*(3), 785-793.

Cosentino, A., & Giacobbe, S. (2006). Shell, Ornament In Pinna Nobilis And Pinna Ruidis. *Journal of Conchology*, *39*(2), 135.

Coppa, S., de Lucia, G. A., Magni, P., Domenici, P., Antognarelli, F., Satta, A., & Cucco, A. (2013). The effect of hydrodynamics on shell orientation and population density of Pinna nobilis in the Gulf of Oristano (Sardinia, Italy). *Journal of Sea Research*, *76*, 201-210.

Cuif, J. P., Denis, A., Flamand, D., & Frérotte, B. (1985). Etude ultrastructurale de la transition prismes/nacre dans filetest de Pinna nobilis L (mollusque, lamellibranche). *Sci Rep Port Cros natl Park Fr*, *11*, 95-107.

Dekshenieks, M. M., Hofmann, E. E., Klinck, J. M., & Powell, E. N. (2000). Quantifying the effects of environmental change on an oyster population: a modeling study. *Estuaries*, *23*(5), 593.

Delgado, M. (1987). Fitoplancton de las balitas del delta del Ebro.

Fasola, M., & Ruiz, X. (1996). The value of rice fields as substitutes for natural wetlands for waterbirds in the Mediterranean region. *Colonial waterbirds*, 122-128.

Garcés E., Delgado M., Masó M., et al. 1999. In situ growth rate and distribution of the ichthyotoxic dinoflagellate *Gyrodinium corsicum* Paulmier in an estuarine embayment (Alfaques Bay, NW Mediterranean Sea)

García March, J. R. (2005). Aportaciones al conocimiento de la biología de Pinna Nobilis Linneo, 1758 (Mollusca bivalvia) en el litoral mediterráneo ibérico.

García-March, J. R., & Kersting, D. K. (2006, July). Preliminary data on the distribution and density of Pinna nobilis and Pinna rudis in the Columbretes Islands Marine Reserve (Western Mediterranean, Spain). In *International Congress on Bivalvia, Universitat Autònoma de Barcelona, Bellaterra, Catalunya, Spain July* (pp. 22-27).

García-March, J. R., Manuel García-Carrascosa, A., & Luís Peña, Á. (2002). In situ measurement of Pinna nobilis shells for age and growth studies: a new device. *Marine ecology*, *23*(3), 207-217.

Garcia-March, J. R., & Márquez-Aliaga, A. (2007). Pinna nobilis L., 1758 age determination by internal shell register. *Marine Biology*, *151*(3), 1077-1085.

Garcia-March, J. R., Marquez-Aliaga, A., Wang, Y. G., Surge, D., & Kersting, D. K. (2011). Study of Pinna nobilis growth from inner record: How biased are posterior adductor muscle scars estimates. *Journal of experimental marine biology and ecology*, *407*(2), 337-344.

García-March, J. R., Pérez-Rojas, L., & García-Carrascosa, A. M. (2007). Influence of hydrodynamic forces on population structure of Pinna nobilis L., 1758 (Mollusca: Bivalvia): The critical combination of drag force, water depth, shell size and orientation. *Journal of Experimental Marine Biology and Ecology*, *342*(2), 202-212.

Guallart, J., & Templado, J. (2012). Pinna nobilis. En: VV. AA., Bases ecológicas preliminares para la conservación de las especies de interés comunitario en España: Invertebrados.

Hendriks, I. E., Basso, L., Deudero, S., Cabanellas-Reboredo, M., & Álvarez, E. (2012). Relative growth rates of the noble pen shell Pinna nobilis throughout ontogeny around the Balearic Islands (Western Mediterranean, Spain). *Journal of Shellfish Research*, *31*(3), 749-756.

Ibàñez, C. (1997). Pla XXI: Directius per a la conservacio i el desenvolupment sostenible al delta de l'Ebre (Plan XXI: Guidelines for conservation and sustainable development in the Ebro Delta).

Ibàñez, C., Prat, N., & Canicio, A. (1996). Changes in the hydrology and sediment transport produced by large dams on the lower Ebro river and its estuary. *Regulated Rivers: Research & Management*, *12*(1), 51-62.

Rabaoui, L., Zouari, S. T., Katsanevakis, S., & Hassine, O. K. B. (2007). Comparison of absolute and relative growth patterns among five Pinna nobilis populations along the Tunisian coastline: an information theory approach. *Marine Biology*, *152*(3), 537-548.)

Katsanevakis, S. (2006). Modelling fish growth: model selection, multi-model inference and model selection uncertainty. *Fisheries Research*, *81*(2), 229-235.

Katsanevakis, S. (2007b). Growth and mortality rates of the fan mussel Pinna nobilis in Lake Vouliagmeni (Korinthiakos Gulf, Greece): a generalized additive modelling approach. *Marine Biology*, *152*(6), 1319-1331.

Kennedy, V. S., Newell, R. I., & Eble, A. F. (Eds.). (1996). *The eastern oyster: Crassostrea virginica*. University of Maryland Sea Grant College.

Kožul, V., Glavić, N., Bolotin, J., & Antolović, N. (2012). Growth of the fan mussel Pinna nobilis (Linnaeus, 1758)(Mollusca: Bivalvia) in experimental cages in the South Adriatic Sea. *Aquaculture Research*, *44*(1), 31-40.

Llebot, C., Rueda, F. J., Solé, J., Artigas, M. L., & Estrada, M. (2014). Hydrodynamic states in a wind-driven microtidal estuary (Alfaques Bay). *Journal of sea research*, *85*, 263-276.

Lowenstam, H. A., & Weiner, S. (1989). *On biomineralization*. Oxford University Press on Demand.

Mañosa, S., Mateo, R., & Guitart, R. (2001). A review of the effects of agricultural and industrial contamination on the Ebro delta biota and wildlife. *Environmental Monitoring and Assessment*, *71*(2), 187-205.

Marin, F., & Luquet, G. (2005). Molluscan biomineralization: The proteinaceous shell constituents of Pinna nobilis L. *Materials Science and Engineering: C*, *25*(2), 105-111.

Marin, F., Narayanappa, P., & Motreuil, S. (2011). Acidic shell proteins of the mediterranean fan mussel Pinna nobilis. In *Molecular Biomineralization* (pp. 353-395). Springer Berlin Heidelberg.

Mihailinovic, M. (1955). Orijentacioni podaci o brzini rastenja losture. *Morsko ribarstvo*, *7*(9), 238.

Moreteau, J. C., & Vicente, N. (1982). EVOLUTION OF A POPULATION OF PINNA-NOBILIS L (MOLLUSCA, BIVALVI). *Malacologia*, *22*(1-2), 341-345.

Newell, C. R., & Hidu, H. (1982). The effects of sediment type on growth rate and shell allometry in the soft shelled clam Mya arenaria L. *Journal of Experimental Marine Biology and Ecology*, *65*(3), 285-295.

Paynter, K. T., & Dimichele, L. (1990). Growth of tray-cultured oysters (Carssostrea virginica Gmelin) in Chesapeake Bay. *Aquaculture*, *87*(3-4), 289-297.

Paynter, K. T., & Burreson, E. M. (1991). Effects of Perkinsus marinus infection in the eastern oyster, Crassostrea virginica: II. Disease development and impact on growth rate at different salinities. *J. Shellfish Res*, *10*(2), 425-431.

Phillips, N. E. (2005). Growth of filter-feeding benthic invertebrates from a region with variable upwelling intensity. *Marine Ecology Progress Series*, *295*, 79-89.

Porri, F., Jordaan, T., & McQuaid, C. D. (2008). Does cannibalism of larvae by adults affect settlement and connectivity of mussel populations. *Estuarine, Coastal and Shelf Science*, *79*(4), 687-693.

Prado, P., Caiola, N., & Ibáñez, C. (2014). Habitat use by a large population of Pinna nobilis in shallow waters. *Scientia Marina*, *78*(4), 555-565.

Rabaoui, L., Tlig-Zouari, S., Katsanevakis, S., Belgacem, W., & Hassine, O. K. B. (2011). Differences in absolute and relative growth between two shell forms of Pinna nobilis (Mollusca: Bivalvia) along the Tunisian coastline. *Journal of sea research*, *66*(2), 95-103.

Rabaoui, L., Zouari, S. T., Katsanevakis, S., & Hassine, O. K. B. (2007). Comparison of absolute and relative growth patterns among five Pinna nobilis populations along the Tunisian coastline: an information theory approach. *Marine Biology*, *152*(3), 537-548.

Richardson, C. A., Kennedy, H., Duarte, C. M., Kennedy, D. P., & Proud, S. V. (1999). Age and growth of the fan mussel Pinna nobilis from south-east Spanish Mediterranean seagrass (Posidonia oceanica) meadows. *Marine Biology*, *133*(2), 205-212.

Shumway, S. E. (1996). Natural environmental factors. *The eastern oyster Crassostrea virginica*, *467513*.

Siletic, T., & Peharda, M. (2003). Population study of the fan shell Pinna nobilis L. in Malo and Veliko Jezero of the Mljet National Park (Adriatic Sea). Scientia Marina, 67(1), 91-98.

Silina, A. V. (2011). Comparison of bivalves of Family Pinnidae from Southern Vietnam: A morphometric approach. *The Korean Journal of Malacology*, *27*(4), 345-351.

Solé, J., Turiel, A., Estrada, M., Llebot, C., Blasco, D., Camp, J., ... & Diogène, J. (2009). Climatic forcing on hydrography of a Mediterranean bay (Alfaques Bay). *Continental Shelf Research*, *29*(15), 1786-1800.

Steffani C.N. & Branch G.M. (2003) Growth rate, condition, and shell shape of Mytilus galloprovincialis: responses to wave exposure. Marine Ecology Progress Series 246, 197–209.

Taylor, J. D., & Kennedy, W. J. (1969). The influence of the periostracum on the shell structure of bivalve molluscs. *Calcified Tissue International*, *3*(1), 274-283.

Urey, H. C. (1947). The thermodynamic properties of isotopic substances. *Journal of the Chemical Society (Resumed)*, 562-581.

Vicente, N. (1990). Estudio ecológico y protección del molusco lamelibranquio Pinna nobilis L. 1758 en la costa mediterránea. *Iberus*, *9*(1-2), 269-279.

Vicente, N., & Moreteau, J. C. (1991). Statut de Pinna nobilis L. en Mediterranee (mollusque eulamellibranche). *Les espèces marines à protéger en Méditerranée*, 159-168.

Vidondo, B., Duarte, C. M., Middelboe, A. L., Stefansen, K., Lützen, T., & Nielsen, S. L. (1997). Dynamics of a landscape mosaic: size and age distributions, growth and demography of seagrass Cymodocea nodosa patches. *Marine Ecology Progress Series*, 131-138.

Von Bertalanffy, L. (1938). A quantitative theory of organic growth (inquiries on growth laws. II). *Human biology*, *10*(2), 181-213.

Wefer, G., & Berger, W. H. (1991). Isotope paleontology: growth and composition of extant calcareous species. *Marine geology*, *100*(1-4), 207-248.

Wise Jr, S. W. (1970). Microarchitecture and mode of formation of nacre (mother of pearl) in pelecypods, gastropods and cephalopods. *Eclogae Geologicae Helvetiae*, *63*, 775-797.

Zakhama-Sraieb, R., Sghaier, Y. S., Omrane, A., & Charfi Cheikhrouha, F. (2011). Density and population structure of Pinna nobilis (Mollusca, Bivalvia) in the Ghar El Melh lagoon (NE Tunisia).

Zavodnik, D. (1967). Contribution to the ecology of Pinna nobilis L. *Mollusca: Bivalvia) in the Northern Adriatic Sea. Thalassia Yugoslavica*, *3*, 93-102.

Zavodnik et al., 1991 Zavodnik, D., Hrs-Brenko, M., & Legac, M. (1991). Synopsis on the fan shell Pinna nobilis L. in the eastern Adriatic Sea. *Les espèces marines à protéger en Méditerranée*, 169-178.